AD A130454

R-RRA-S-3-28-73

AD

MATHEMATICAL MODELS
FOR
ENGINEERING ANALYSIS AND DESIGN
OF
HOWITZER, LIGHT, TOWED: 105MM SOFT RECOIL, XM204

2

TECHNICAL REPORT

BY

MICHAEL C. NERDAHL
&
JERRY W. FRANTZ

MAY 1973

ARTILLERY WEAPON SYSTEMS DIRECTORATE

WEAPONS LABORATORY - RIA

Rock Island, Illinois 61201

~~DISTRIBUTION~~

~~Distribution limited to U. S. Government agencies only; Test & Evaluation of Military Hardware presented; May 1973. Other requests for this document must be referred to Artillery Weapons Systems Directorate, U. S. Army Weapons Command.~~

The findings in this report are not to be construed as an official Department of the Army position, unless so designated by other authorized documents.

DISPOSITION INSTRUCTIONS

Destroy this report when it is no longer needed. Do not return it to the originator.

ARTILLERY WEAPON SYSTEMS DIRECTORATE
WEAPONS LABORATORY - ROCK ISLAND
U. S. ARMY WEAPONS COMMAND

TECHNICAL REPORT

R-RRA-S-3-28-73

MATHEMATICAL MODELS FOR ENGINEERING ANALYSIS AND DESIGN OF HOWITZER, LIGHT, TOWED; 105MM SOFT RECOIL, XM204

By

Michael C. Nerdahl
Advanced Systems Division
Artillery Weapon Systems Directorate

and

Jerry W. Frantz
Systems Performance Division
Research Directorate

May 1973

D. A. Project No. 1-W-5-63608-D-376

DISTRIBUTION:

~~Distribution limited to U. S. Government agencies only; Test and Evaluation of military hardware presented; May 1973. Other requests for this document must be referred to Artillery Weapon Systems Directorate, Rock Island Weapons Laboratory.~~

ABSTRACT

Mathematical models used in design of the XM204 Howitzer (AD and ED Prototypes) are described in this report. The physical basis for the mathematical representation is presented along with the derivation of the required equations. While these models have been generalized to allow their use in other weapon design situations, some modification will be necessary to include features not specifically considered. Systems of equations which will provide for the definition of required control functions as well as the prediction of recoil mechanism functioning and weapon motions are summarized.

FOREWORD

This project was authorized under AMCMS Code 553G.12.42710.01. The work was funded under DA Project No. 1-W-5-63608-D-376.

Suggestions and requests by the members of the XM204 design team served as the basis for the mathematical representations of the weapon and their support is hereby acknowledged.

CONTENTS

Page

ABSTRACT... ii

FOREWORD... ii

INTRODUCTION....................................... 1

CONCLUSIONS & RECOMMENDATIONS...................... 3

RIGID BODY MODEL OF A SOFT RECOIL MECHANISM........ 7

DESIGN OF RECOIL & COUNTERRECOIL CONTROL ORIFICE... 22

DEFINITION OF RECOIL & COUNTERRECOIL CONTROL

FUNCTIONS.. 26

CARRIAGE RESPONSE TO FIRING LOADS.................. 39

EVALUATION OF DYNAMIC REACTIONS.................... 66

EVALUATION OF STATIC REACTIONS..................... 75

REFERENCES... 79

SYMBOL TABLE....................................... 80

APPENDIX... 88

DISTRIBUTION....................................... 92

LIST OF ILLUSTRATIONS

Figure No.	Title	Page
1	Comparison of Recoil Cycles	1
2	Schematic Diagram of Soft Recoil Mechanism	4
3	Free Body Diagram of Floating Piston	5
4	Free Body Diagram of Piston Rod	5
5	Relative Position of Buffer and Piston During Engagement	6
6	Fluid Flow Diagram	6
7	Free Body Diagram of Recoiling Mass	26
8	Assumed Force System for a Conventional Recoil Cycle	28
9	Assumed Force System for an Ideal Soft Recoil Cycle	29
10	Counterrecoil Control Function	33
11	Schematic Representation of a Soft Recoil Howitzer	38
12	Free Body Diagrams of Recoiling Mass and Cradle	40
13	Spring Equilibrator - Compression Type	54
14	Schematic Diagram of Elevation Strut	56
15	Load Deflection Curve for One Elevation Strut	57
16	Free Body Diagram of Carriage	72
A-1	Schematic Diagram of Forward Buffer	91

INTRODUCTION

The recoil mechanism of an artillery weapon provides a controlled resistance to some allowable motion of the recoiling parts. Consequently, the major portion of the weapon structure is protected from the total breech force and the ground reactions are limited. In a conventional recoil cycle, motion is initiated by application of the breech force. The resisting force may be provided by deflection of a spring, by fluid flow through an orifice or by both of these. In the soft-recoil cycle, the recoiling parts are first accelerated in the direction of projectile travel. Application of the breech force (i.e., by ignition of the propellant primer) is delayed until a predetermined velocity has been attained. The breech force then reverses the motion of the recoiling mass and the recoiling parts are returned to their initial (battery or latch) position. A comparison of conventional and soft-recoil cycles is shown in Figure 1.

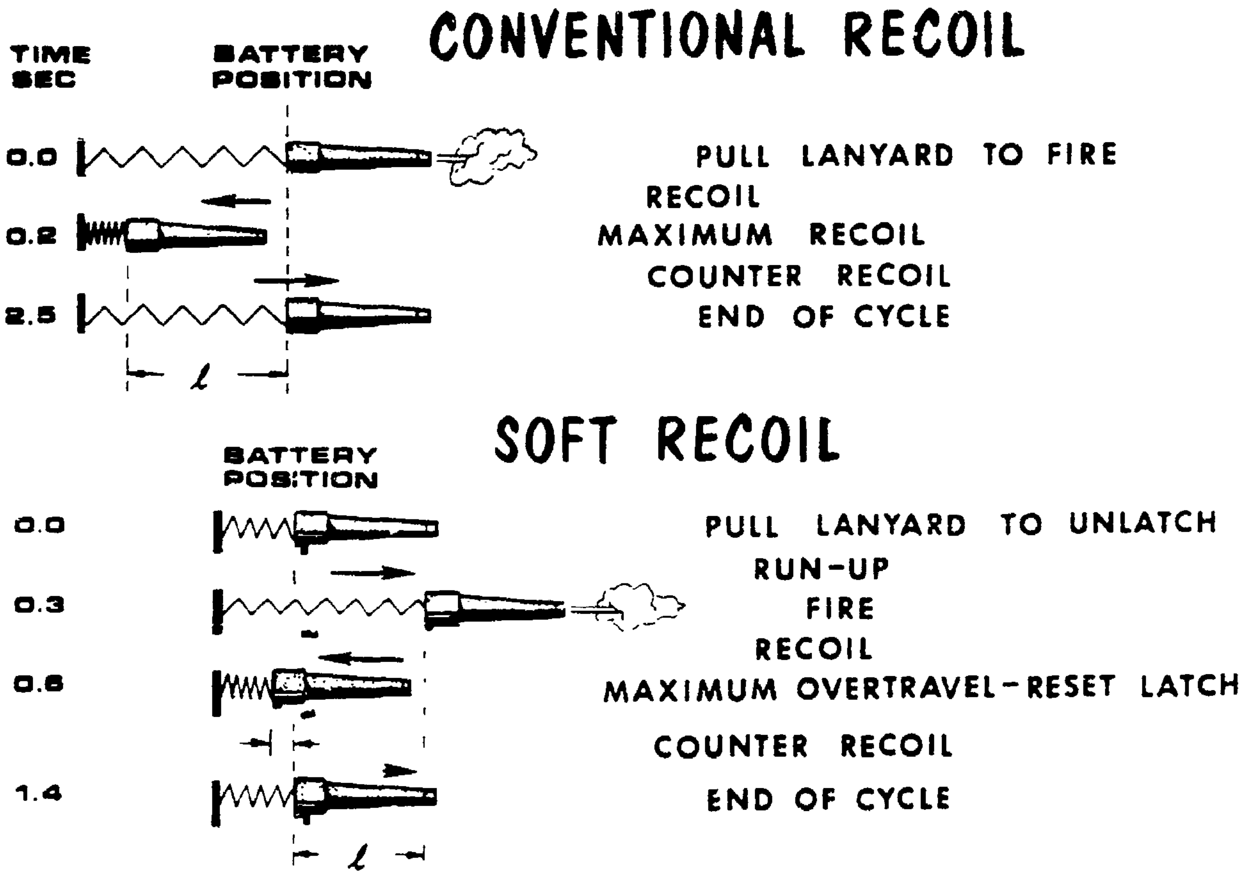

FIGURE 1

Comparison of Recoil Cycles

Development of a reliable soft-recoil mechanism for modern artillery began in 1957 with the modification of an M101 Howitzer, 105mm. While evaluation tests of this modified weapon demonstrated the feasibility and value of a soft-recoil system, mechanism reliability was unacceptable. (Reference 1). In March 1964, design and fabrication of an experimental firing fixture having an improved recoil mechanism was initiated. Extensive firing tests of this fixture were conducted to confirm feasibility of this weapon concept, to determine accuracy and durability characteristics, and to identify and examine functional problems. (References 2 & 3).

In 1968, funding was provided for design and manufacture of a preprototype howitzer incorporating a soft-recoil mechanism. This weapon was designated as the Howitzer, Light, Towed: 105mm, Soft Recoil, XM204. The major components were the XM205 Cannon, the XM46 Recoil Mechanism, and the XM44 Carriage. Design parameters for the first prototype were based on firing of the XM606 (28.5 pounds) projectile with the M85 charge (Zones 3 through 8) and the standard M1 (33 pound) projectile with the M67 charge (Zones 1 through 7). Safety Certification Tests were conducted at Aberdeen Proving Ground in early 1970. Military Potential Tests, performed at Fort Sill, Oklahoma, were successfully completed in December 1970. Both standard 105mm howitzers (M101A1 and M102) were used for comparison during these tests. Stability, accuracy, and human engineering characteristics of the XM204 were favorably commented upon by the user. In all, 2,269 rounds were fired from this MPT weapon with 413 at the maximum impulse level. (Zone 8). (References 4, 5, and 6).

Mathematical models of the weapon were developed to aid the design engineers in establishing and evaluating physical configuration, structural integrity and functional controls. (References 7, 8 & 9). These models were used to verify designs and to systematically study the effects of parametric variation before selection of specific values.

In the early part of 1972, the design of the XM205 Cannon was changed to permit test firing of the XM200 supercharge. This longer and heavier tube was installed on the original prototype. Concurrently, a new velocity sensor, an improved suspension system, ring spring assemblies in the elevation struts, and a relocated firing base were incorporated. (Reference 10). With fabrication and installation of a new cradle, this modified weapon became an Advanced Development Prototype.

Design of the Engineering Development Prototypes that will be used for DT II/OT II has been initiated. As a result of the changes in the cannon and the increase in ammunition impulse levels, new recoil and counterrecoil orifice designs were required and the effect of carriage flexibility had to be reassessed. Consequently, the original mathematical models were modified to more closely represent the current design configuration. At the same time, an attempt was made to generalize the form so that minor alterations would allow for their use in the analysis of future soft-recoil weapon concepts.

CONCLUSIONS AND RECOMMENDATIONS

While the models presented in this report were being developed, the primary considerations were choice of significant motions and physical characteristics of the weapon. Specific design features and functional characteristics peculiar to the XM204 Howitzer have been included to adapt the models to the requirements of the design team. These models are intended to provide a reasonable representation of normal firing cycles based on firing of the standard zoned charges and of abnormal cycles resulting from a cook-off or from a misfire.

Test plans include the collection of data from the firing of the Advanced Development Prototype under various conditions. Comparison of test data and predictions obtained from the mathematical models will provide a basis for model validation. The models should then be used to identify critical design parameters, to define the effect of parameter variations, and to establish required values for specific parameters for use in design of the Engineering Development Prototypes.

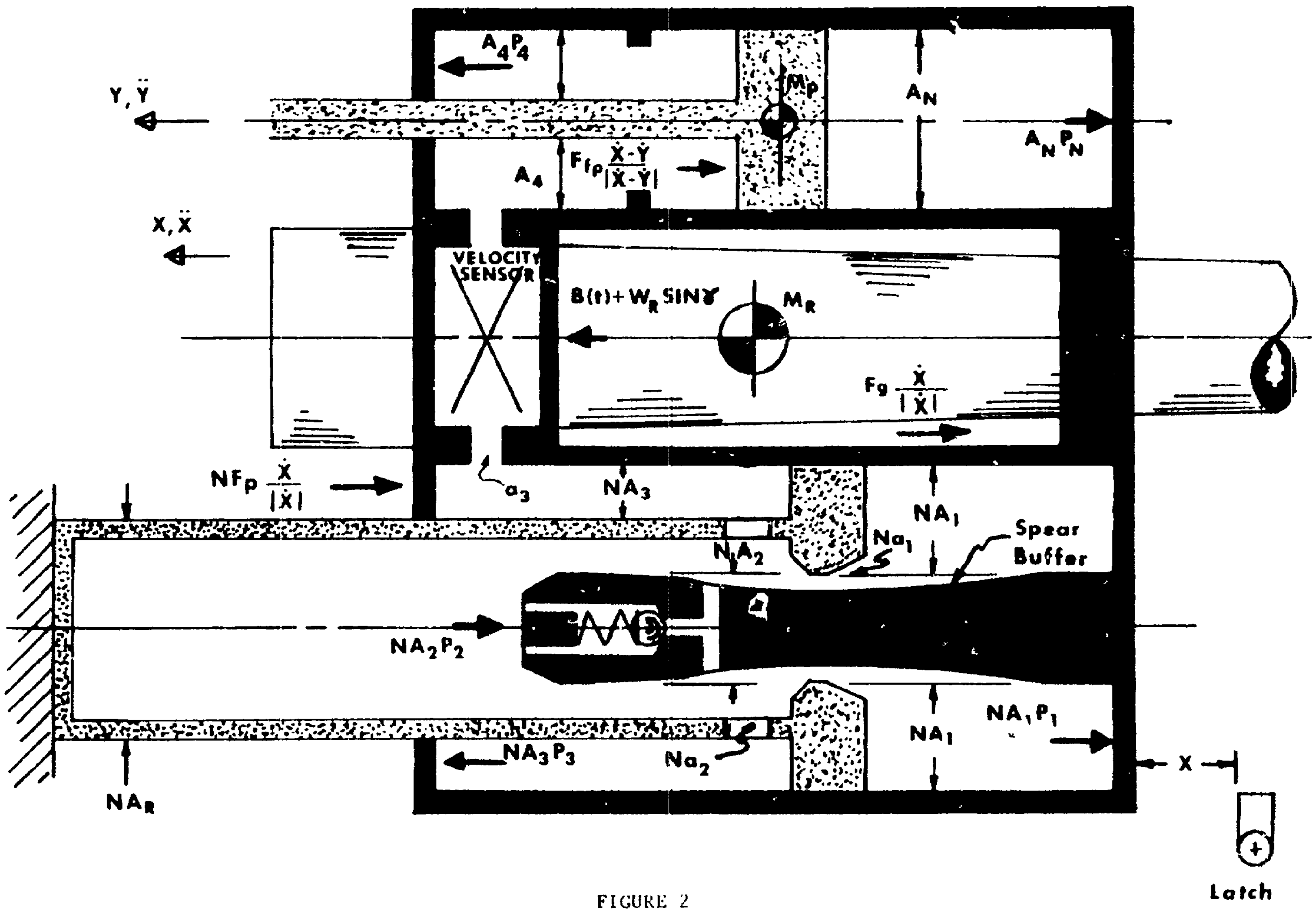

FIGURE 2

Schematic Diagram of Soft Recoil Mechanism
Showing Forces on Recoiling Parts

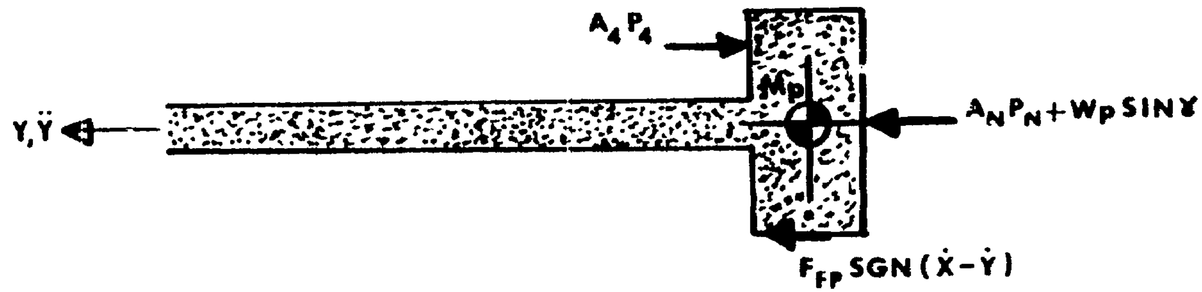

FIGURE 3

Free Body Diagram of Floating Piston

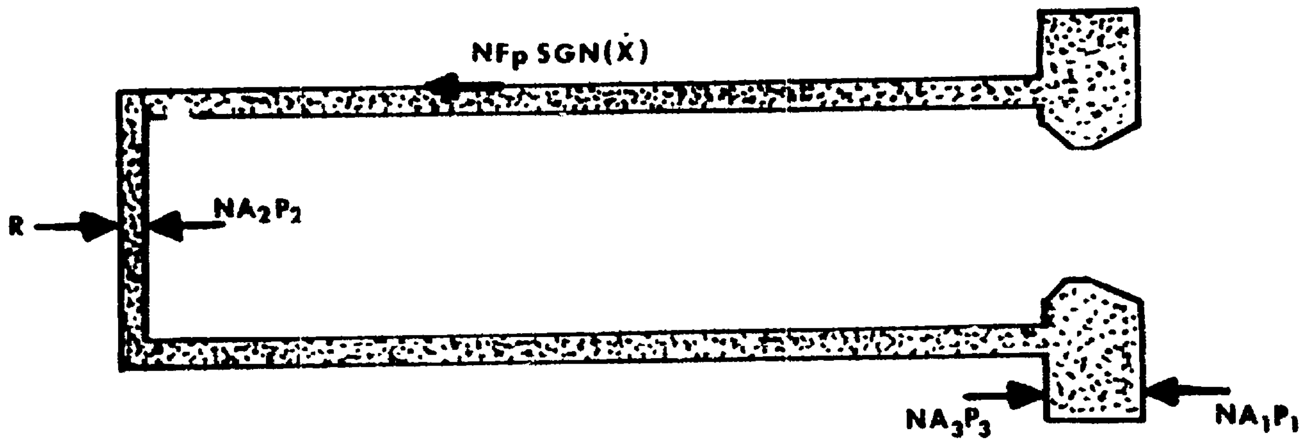

FIGURE 4

Free Body Diagram of Piston Rod

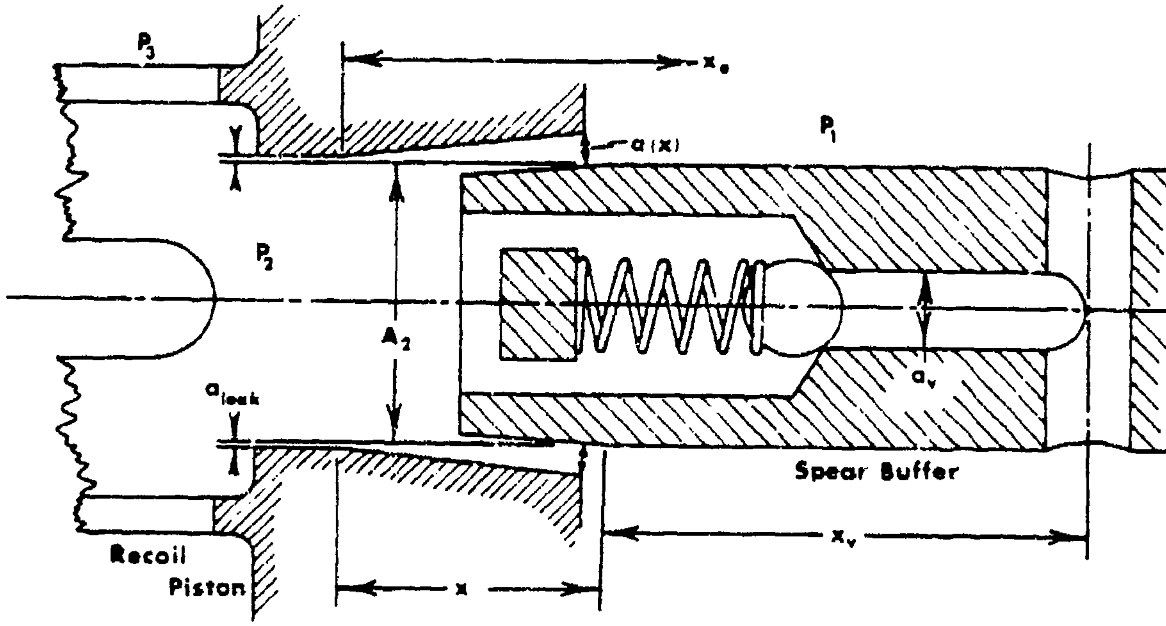

Figure 5
Relative Position of Buffer and Piston During Engagement
(As shown, $x < 0$ For $x > x_e$, $a_1 < A_2$; For $x \leq x_e$, $a_1 = A_2$)

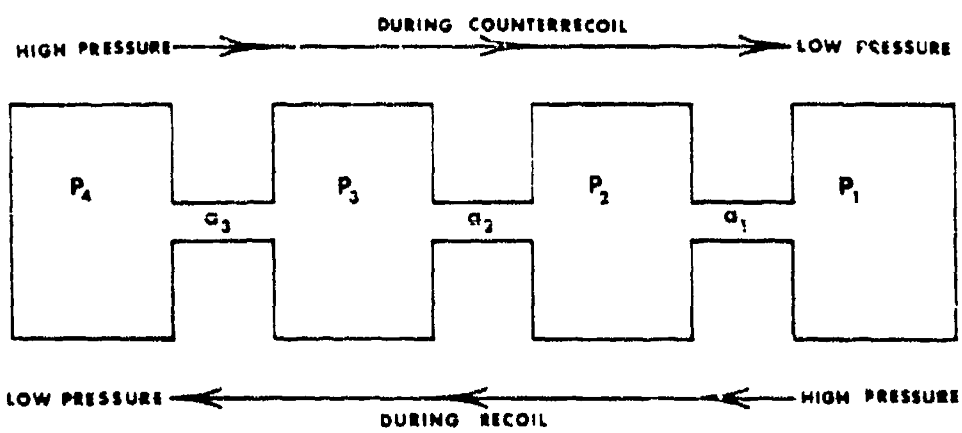

Figure 6
Fluid Flow Diagram

RIGID BODY MODEL OF A SOFT RECOIL MECHANISM

The schematic diagram of the soft recoil mechanism (Figure 2) and the free body diagrams (Figures 2, 3, and 4) are the basis for the mathematical model of recoil motion used to predict fluid flow and its control. Conventionally, the breech force is assumed to cause positive acceleration. Therefore, the displacements "x", "y" and "x - y" increase in magnitude for the force system shown. With the recoiling parts in their initial or battery position, the variables "x" and "y" are defined as zero. (Note that "$x \gg y \gg 0$" in Figure 2 - i.e., rearward displacement). Symbols used in deriving the equations used to predict system motion and functioning are defined in the Symbol Table (Page 80).

The spear buffer shown in Figure 2 is required to protect the system from the overload which would be caused by the firing of the maximum impulse charge before imparting a forward motion to the recoiling parts (as in the case of a cook-off). This spear buffer restricts fluid flow between the pressures P_1 and P_2 during part of the cycle. As illustrated schematically in Figure 5, this restriction exists while

$$x_{max} > x > x_e$$

with "x_e" being the value of "x" for which a_1 becomes equal to A_2 .

For any "x", the flow diagram is shown in Figure 6 with flow from P_1 to P_4 when "x" is increasing (defined as recoil). The direction of flow is reversed when "x" is decreasing (during run-up and during counterrecoil). Values for the orifice areas (a_i's) will vary with direction of fluid flow, position of the spear buffer relative to the piston, and functioning of the velocity sensor.

The pressure drop across the "ith" orifice is defined as

$$(1) \qquad g(v_i) = \frac{\sigma}{2g}\left(\frac{v_i}{c_i}\right)^2 \operatorname{sgn}(v_i)$$

Then,

$$(2) \qquad P_1 - P_2 = g(v_1)$$

$$(3) \qquad P_2 - P_3 = g(v_2)$$

$$(4) \qquad P_3 - P_4 = g(v_3)$$

where

σ = fluid density

g = acceleration due to gravity

c_i = discharge coefficient for "ith" orifice

v_i = fluid velocity through "ith" orifice

$\mathrm{sgn}(v_i)$ = algebraic sign of v_i

With fluid flow restricted by the spear buffer (that is, for "$x \geq x_e$"),

$$NA_1\dot{x} = Na_1v_1$$

$$(5) \qquad v_1 = \frac{A_1}{a_1} \dot{x}$$

$$Na_1v_1 + NA_2\dot{x} = Na_2v_2$$

$$NA_1\dot{x} + NA_2\dot{x} = Na_2v_2$$

$$(6) \qquad v_2 = \frac{A_1 + A_2}{a_2} \dot{x}$$

$$Na_2v_2 = NA_3\dot{x} + a_3v_3$$

$$a_3v_3 = NA_1\dot{x} + NA_2\dot{x} - NA_3\dot{x} = NA_R\dot{x}$$

$$(7) \qquad v_3 = \frac{NA_R}{a_3} \dot{x}$$

Now,

$$a_3 v_3 = A_4(\dot{x} - \dot{y})$$

$$NA_R \dot{x} = A_4 \dot{x} - A_4 \dot{y}$$

$$(8) \quad \dot{y} = \frac{A_4 - NA_R}{A_4} \dot{x}$$

$$(9) \quad \ddot{y} = \frac{A_4 - NA_R}{A_4} \ddot{x}$$

$$(10) \quad y = \frac{A_4 - NA_R}{A_4} x$$

These relations hold as long as the system remains completely filled with fluid. (Monitoring of computed pressure values to ensure that they remain positive will demonstrate the existence of an oil filled system).

Rearranging Equations 2, 3, and 4

$$(11) \quad P_3 = P_4 + g(v_3)$$

$$(12) \quad P_2 = P_3 + g(v_2) = P_4 + g(v_2) + g(v_3)$$

$$(13) \quad P_1 = P_2 + g(v_1) = P_4 + g(v_1) + g(v_2) + g(v_3)$$

From the free body diagrams (Figures 2 and 3), with "$x \gg x_d$" (spear buffer restricting fluid flow)

$$(14) \quad M_R \ddot{x} = B(t) + W_R \sin \gamma - NF_p \operatorname{sgn}(\dot{x}) - F_{fp} \operatorname{sgn}(\dot{x} - \dot{y}) - F_g \operatorname{sgn}(\dot{x}) - A_N P_N + A_4 P_4 + NA_3 P_3 - NA_2 P_2 - NA_1 P_1$$

and

$$(15)\quad M_p \ddot{y} = W_p \sin \gamma + A_N P_N + F_{fp} \operatorname{sgn}(\dot{x} - \dot{y}) - A_4 P_4$$

Noting that $\operatorname{sgn}(\dot{x}) = \operatorname{sgn}(\dot{x} - \dot{y})$ and substituting for $\ddot{y}$ (Equation 9), Equations 14 and 15 are rewritten as

$$(14.1)\quad M_R \ddot{x} = B(t) + W_R \sin \gamma - (NF_p + F_g + F_{fp}) \operatorname{sgn}(\dot{x})$$

$$- A_N P_N + A_4 P_4 + NA_3 P_3 - NA_2 P_2 - NA_1 P_1$$

$$(15.1)\quad M_p \left[\frac{A_4 - NA_R}{A_4}\right] \ddot{x} = W_p \sin \gamma + A_N P_N + F_{fp} \operatorname{sgn}(\dot{x}) - A_4 P_4$$

By adding Equations 14.1 and 15.1, one obtains

$$(16)\quad \left[M_R + \left(\frac{A_4 - NA_R}{A_4}\right) M_p\right] \ddot{x} = B(t) + (W_R + W_p) \sin \gamma$$

$$- (NF_p + F_g) \operatorname{sgn}(\dot{x})$$

$$+ NA_3 P_3 - NA_2 P_2 - NA_1 P_1$$

By substituting Equations 11, 12 and 13, Equation 16 may be rewritten as

$$\left[M_R + \left(\frac{A_4 - NA_R}{A_4}\right) M_p\right] \ddot{x} = B(t) + (W_R + W_p) \sin \gamma$$

$$- (NF_p + F_g) \operatorname{sgn}(\dot{x}) + NA_3 P_4$$

$$+ NA_3\, g(v_3) - NA_2 P_4 - NA_2\, g(v_2)$$

$$- NA_2\, g(v_3) - NA_1 P_4 - NA_1\, g(v_1)$$

$$- NA_1\, g(v_2) - NA_1\, g(v_3)$$

Collecting terms

$$\left[M_R + \left(\frac{A_4 - NA_R}{A_4}\right) M_p\right]\ddot{x} = B(t) + (W_R + W_p)\sin\gamma$$

$$- (NF_p + F_g)\,\mathrm{sgn}(\dot{x})$$

$$- N(A_1 + A_2 - A_3)\,P_4$$

$$- NA_1\,g(v_1) - N(A_1 + A_2)\,g(v_2)$$

$$- N(A_1 + A_2 - A_3)\,g(v_3)$$

Solving Equation 15.1 for P_4,

$$(15.2)\quad P_4 = \frac{1}{A_4} W_p \sin\gamma + \frac{1}{A_4} F_{fp}\,\mathrm{sgn}(\dot{x})$$

$$+ \frac{A_N}{A_4} P_N - \frac{M_p}{A_4}\left[\frac{A_4 - NA_R}{A_4}\right]\ddot{x}$$

By substitution, (noting that $A_R = A_1 + A_2 - A_3$)

$$\left[M_R + \left(\frac{A_4 - NA_R}{A_4}\right) M_p\right]\ddot{x} = B(t) + (W_R + W_p)\sin\gamma$$

$$- (NF_p + F_g)\,\mathrm{sgn}(\dot{x}) - \frac{NA_R}{A_4} W_p \sin\gamma$$

$$- \frac{NA_R}{A_4} F_{fp}\,\mathrm{sgn}(\dot{x}) - \frac{NA_R A_N}{A_4} P_N$$

$$- \frac{NA_R M_p}{A_4}\left[\frac{A_4 - NA_R}{A_4}\right]\ddot{x}$$

$$- NA_1\,g(v_1) - N(A_1 + A_2)\,g(v_2) - NA_R\,g(v_3)$$

or, rearranging terms

$$(17) \quad \left[M_R + \left(\frac{A_4 - NA_R}{A_4}\right)^2 M_p\right] \ddot{x} = B(t) + \left[W_R + \left(\frac{A_4 - NA_R}{A_4}\right) W_p\right] \sin \gamma$$

$$- \left(NF_p + F_g + \frac{NA_R}{A_4} F_{fp}\right) \operatorname{sgn}(\dot{x}) - \frac{NA_R A_N}{A_4} P_N$$

$$- NA_1\, g(v_1) - N(A_1 + A_2)\, g(v_2) - NA_R\, g(v_3)$$

If the initial value is V_o, the gas volume for any displacement "x" is written as

$$V_N = V_o - A_N (x - y) = V_o - A_N \frac{NA_R}{A_4} x$$

Then, assuming adiabatic gas laws, the gas pressure for any displacement "x" is determined from

$$P_N V_N^{\ k} = P_o V_o^{\ k}$$

$$P_N = P_o \left(\frac{V_o}{V_N}\right)^k$$

$$(18) \quad P_N = P_o \left(\frac{V_o}{V_o - \frac{NA_R A_N}{A_4} x}\right)^k$$

From the free body diagram (Figure 4), the force on the recoil rod is given by

$$(19) \quad R = NA_1 P_1 + NA_2 P_2 - NA_3 P_3 + NF_p \operatorname{sgn}(\dot{x})$$

When fluid flow is not restricted by the spear buffer, (i.e. for "$x < x_e$"), the preceding analysis must be modified by noting that the force on the end of the spear buffer (Figure 2) will be NA_2P_1 rather than NA_2P_2 and that flow from P_1 to P_2 will be defined by

$$N(A_1 + A_2)\, \dot{x} = Na_1 v_1$$

$$(5.1) \quad v_1 = \frac{A_1 + A_2}{a_1} \dot{x}$$

Therefore, for "$x < x_e$", Equation 14.1 should be written as

$$M_R\ddot{x} = B(t) + W_R \sin \gamma - (NF_p + F_g + F_{fp}) \operatorname{sgn}(\dot{x}) \tag{14.2}$$

$$- A_N P_N + A_4 P_4 + NA_3 P_3 - NA_2 P_1 - NA_1 P_1$$

when this is added to Equation 15.1, one obtains

$$\left[M_R + \left(\frac{A_4 - NA_R}{A_4}\right) M_p\right] \ddot{x} = B(t) + (W_R + W_p) \sin \gamma \tag{16.1}$$

$$- (NF_p + F_g) \operatorname{sgn}(\dot{x})$$

$$+ NA_3 P_3 - N(A_1 + A_2) P_1$$

From this, by substituting Equations 11 and 13,

$$\left[M_R + \left(\frac{A_4 - NA_R}{A_4}\right) M_p\right] \ddot{x} = B(t) + (W_R + W_p) \sin \gamma$$

$$- (NF_p + F_g) \operatorname{sgn}(\dot{x})$$

$$+ NA_3 P_4 + NA_3\, g(v_3)$$

$$- N(A_1 + A_2)\, P_4 - N(A_1 + A_2)\, g(v_1)$$

$$- N(A_1 + A_2)\, g(v_2) - N(A_1 + A_2)\, g(v_3)$$

Therefore, collecting terms and noting that $A_R = A_1 + A_2 - A_3$

$$\left[M_R + \left(\frac{A_4 - NA_R}{A_4}\right) M_p\right] \ddot{x} = B(t) + (W_R + W_p) \sin\gamma$$

$$- (NF_p + F_g) \operatorname{sgn}(\dot{x})$$

$$- NA_R P_4 - N(A_1 + A_2)\, g(v_1)$$

$$- N(A_1 + A_2)\, g(v_2) - NA_R\, g(v_3)$$

Again, substituting for P_4 and rearranging,

$$(17.1) \quad \left[M_R + \left(\frac{A_4 - NA_R}{A_4}\right)^2 M_p\right] \ddot{x} = B(t) + \left[W_R + \left(\frac{A_4 - NA_R}{A_4}\right) W_p\right] \sin\gamma$$

$$- \left(NF_p + F_g + \frac{NA_R}{A_4} F_{fp}\right) \operatorname{sgn}(\dot{x})$$

$$- \frac{NA_R A_N}{A_4} P_N$$

$$- N(A_1 + A_2)\,[g(v_1) + g(v_2)]$$

$$- NA_R\, g(v_3)$$

By defining

$$(20) \quad \begin{cases} H = 1 & \text{if } x < x_e \\ H = 0 & \text{if } x \geq x_e \end{cases}$$

Equations 5 and 5.1 may be written as

$$(5.2) \qquad v_1 = \frac{A_1 + HA_2}{a_1} \dot{x}$$

Equations 18 and 18.1 may be written as

$$(17.2) \qquad \left[M_R + \left(\frac{A_4 - NA_R}{A_4} \right)^2 M_p \right] \ddot{x} = B(t) - \frac{NA_R A_N}{A_4} P_N$$

$$+ \left[W_R + \left(\frac{A_4 - NA_R}{A_4} \right) W_p \right] \sin \gamma$$

$$- (NF_p + F_g + \left(\frac{NA_R}{A_4} \right) F_{fp}) \operatorname{sgn}(\dot{x})$$

$$- N(A_1 + HA_2)\ g(v_1)$$

$$- N(A_1 + A_2)\ g(v_2)$$

$$- NA_R\ g(v_3)$$

Then, by using Equations 5.2 and 18.2 along with Equation 20, a single system of equations defines the entire cycle as long as the mechanism remains filled with fluid.

Negative pressure values obtained during the solution of the preceding system of equations will denote that the system is no longer completely filled with fluid. If this occurs, a new set of equations is required. This condition is anticipated since fluid flow through the velocity sensor (orifice area a_3) is sharply restricted after initiation of firing to prevent any increase in velocity during an ignition delay period. To approximate system motion after a negative pressure has been computed, assume that

$$P_3 = P_2 = P_1 = 0$$

Then,

$$P_4 = - g(v_3)$$

and Equations 14 and 15 must be rewritten as

$$(21) \qquad M_R \ddot{x} = B(t) + W_R \sin \gamma - (NF_p + F_g) \sin(\dot{x})$$

$$- F_{fp} \operatorname{sgn}(\dot{x} - \dot{y}) - A_N P_N - A_4\ g(v_3)$$

$$(22) \qquad M_p \ddot{y} = W_p \sin \gamma + A_N P_N + F_{fp} \operatorname{sgn}(\dot{x} - \dot{y})$$

$$+ A_4\ g(v_3)$$

with

$$a_3 v_3 = A_4\ (\dot{x} - \dot{y})$$

or

$$(23) \qquad v_3 = \frac{A_4}{a_3} (\dot{x} - \dot{y})$$

and

$$(24) \qquad P_N = P_o \left(\frac{V_o}{V_o - A_N\ (x - y)} \right)^k$$

These equations will be considered as definitions of system motion as long as

$$NA_R\ x > A_4\ (x - y)$$

During this period

$$(25) \qquad R = NF_p \operatorname{sgn}(\dot{x})$$

The governing differential equations of motion are solved by standard numerical methods, with the system controls of the actual mechanism being simulated by logic decisions of the computer. These logic decisions are defined in the following manner.

1. A cycle is initiated by the setting of appropriate initial conditions (e.g., $x = 0$ and $\dot{x} = 0$ at $t = 0$).

2. Firing is initiated on the basis of either velocity (Is "$\dot{x}$" $\geq$ some specified value?) or displacement (Is "x" $\leq$ some specified value?)

3. Ignition delay is simulated by a variation of the time lapse between initiation of firing and application of the breech force.

4. The orifice area a_3 may have either of two values.

$$a_3 = \begin{cases} a_{3bf} & \text{before firing if "}\dot{x} < 0\text{"} \\ a_{3af} & \text{after firing if "}\dot{x} < 0\text{"} \\ a_{3bf} & \text{whenever "}x \quad 0\text{"} \end{cases}$$

5. The orifice area a_2 has a single value for this model.

6. The orifice area a_1 varies with both position and direction of fluid flow, since it is dependent on restriction of fluid flow between P_1 and P_2 by the spear buffer and by functioning of the check valve in the spear buffer. Letting

a_v = flow area through check valve

a_{leak} = annular orifice area resulting from the necessary clearance between the piston head and the spear buffer.

a_x = orifice area which is dependent on position of the spear buffer.

The orifice area may be defined as

$$a_1 = \begin{cases} A_2 + a_{leak} & \text{if} \quad "x < x_e" \\ a_x + a_{leak} + a_v & \text{if} \quad "x_v > x > x_e" \text{ and } "\dot{x} > 0" \\ a_x + a_{leak} & \text{if} \quad "x > x_v" \text{ and } "\dot{x} > 0" \\ a_x + a_{leak} & \text{if} \quad "x > x_e" \text{ and } "\dot{x} < 0" \end{cases}$$

By making "$a_x = A_2$" for "$x < x_e$" the definition simplifies to

$$a_1 = \begin{cases} a_x + a_{leak} & \text{unless} \quad "x_v > x > x_e" \text{ and } "\dot{x} > 0" \\ a_x + a_{leak} + a_v & \text{when} \quad "x_v > x > x_e" \text{ and } "\dot{x} > 0" \end{cases}$$

7. Define

$$H = \begin{cases} 1 & \text{if} \quad "x < x_e" \\ 0 & \text{if} \quad "x \geq x_e" \end{cases}$$

8. Choose governing system of equations on the basis of

$P_3 > 0$ or $P_3 \leq 0$

The rigid body model of the soft recoil mechanism is summarized in Table I.

TABLE I

RIGID BODY MODEL OF SOFT RECOIL MECHANISM

A. EQUATIONS OF MOTION

$\boxed{\text{If } P_3 > 0}$

$$(17.2)\quad \left[M_R + \left(\frac{A_4 - NA_R}{A_4}\right)^2 M_p\right] \ddot{x} = B(t) - \frac{NA_R A_N}{A_4} P_N$$

$$+ \left[W_R + \left(\frac{A_N - NA_R}{A_4}\right) W_p\right] \sin \gamma$$

$$- (NF_p + F_g + \frac{NA_R}{A_4} F_{fp}) \operatorname{sgn}(\dot{x})$$

$$- N(A_1 + HA_2)\, g(v_1) - N(A_1 + A_2)\, g(v_2)$$

$$- NA_R\, g(v_3)$$

$$(20)\quad H = \begin{cases} 1 & \text{if } \text{"}x < x_e\text{"} \\ 0 & \text{if } \text{"}x \geq x_e\text{"} \end{cases}$$

$$(18)\quad P_N = P_o \left(\frac{V_o}{V_o - \frac{NA_R A_N}{A_4} x}\right)^k$$

$$(1)\quad g(v_i) = \frac{\sigma}{2g}\left(\frac{v_i}{c_i}\right)^2 \operatorname{sgn}(v_i)$$

$$(5.2)\quad v_1 = \frac{A_1 + HA_2}{a_1} \dot{x}$$

TABLE I (cont'd)

$$(6) \quad v_2 = \frac{A_1 + HA_2}{a_2} \dot{x}$$

$$(7) \quad v_3 = \frac{A_1 + A_2}{a_3} \dot{x}$$

$$(10) \quad y = \frac{A_4 - NA_R}{A_4} x$$

$$(15.2) \quad P_4 = \frac{1}{A_4} W_p \sin \gamma + \frac{1}{A_4} F_{fp} \operatorname{sgn}(\dot{x}) + \frac{A_N}{A_4} P_N - \frac{M_p}{A_4} \left[\frac{A_4 - NA_R}{A_4}\right] \ddot{x}$$

$$(11) \quad P_3 = P_4 + g(v_3)$$

$$(12) \quad P_2 = P_3 + g(v_2)$$

$$(13) \quad P_1 = P_2 + g(v_1)$$

$$(19) \quad R = NA_1P_1 + NA_2P_2 - NA_3P_3 \pm NF_p \operatorname{sgn}(\dot{x})$$

$$\boxed{\text{If} \quad P_3 < 0 \quad \text{and} \quad NA_R\, x > A_4\,(x - y)}$$

$$(21) \quad M_K \ddot{x} = B(t) + W_R \sin \gamma - (NF_p + F_g) \operatorname{sgn}(\dot{x}) - F_{fp} \operatorname{sgn}(\dot{x} - \dot{y}) - A_N P_N - A_4\, g(v_3)$$

$$(22) \quad M_p \ddot{y} = W_p \sin \gamma + A_N P_N + F_{fp} \operatorname{sgn}(\dot{x} - \dot{y}) + A_4\, g(v_3)$$

$$(23) \quad v_3 = \frac{A_4}{a_3} (\dot{x} - \dot{y})$$

TABLE I (cont'd)

$$(24) \qquad P_N = P_o \left(\frac{V_o}{V_o - A_N (x - y)} \right)^k$$

$$(25) \qquad R = NF_p \, \mathrm{sgn}(\dot{x})$$

B. <u>LOGIC CONTROLS</u>

$$\text{Initiate firing } (t = t_f) \text{ if } \begin{cases} x \leq \text{ firing velocity} \\ \qquad \text{or} \\ x \leq \text{ firing displacement} \end{cases}$$

$$\text{Initiate breech force if } t \geq t_f + \text{Ignition Delay}$$

$$a_3 = \begin{cases} a_{3bf} \text{ whenever } & \dot{x} > 0 \\ a_{3bf} \text{ before firing if } & \dot{x} < 0 \\ a_{3bf} \text{ after firing if } & \dot{x} < 0 \end{cases}$$

$$a_1 = \begin{cases} a_x + a_{leak} \text{ unless } x_v > x > x_e \text{ and } \dot{x} > 0 \\ \\ a_x + a_{leak} + a_v \text{ when } x_v > x > x_e \text{ and } \dot{x} > 0 \end{cases}$$

DESIGN OF RECOIL AND COUNTERRECOIL CONTROL ORIFICE

When $x > 0$, control of recoil motion is provided by the spear buffer. With fluid flow restricted by this component, te motion is defined by

$$(17) \quad \left[M_R + \left(\frac{A_4 + NA_R}{A_4}\right)^2 M_p\right] \ddot{x} = B(t) + \left[W_R + \left(\frac{A_4 - NA_R}{A_4}\right) W_p\right] \sin \gamma$$

$$- (NF_p + F_g + \frac{NA_R}{A_4} F_{fp}) \operatorname{sgn}(\dot{x}) - \frac{NA_R A_N}{A_4} P_N$$

$$- NA_1\, g(v_1) - N(A_1 + A_2)\, g(v_2) - NA_R\, g(v_3)$$

This equation has the form

$$(26) \quad M_{eff}\, \ddot{x} = A(t) - D(t)$$

where

$$(27) \quad M_{eff} = \left[M_R + \left(\frac{A_4 + NA_R}{A_4}\right)^2 M_p\right]$$

$$(28) \quad W_{eff} = \left[W_R + \left(\frac{A_4 - NA_R}{A_4}\right) W_p\right] \sin \gamma$$

$$(29) \quad A(t) = B(t) + W_{eff}$$

$$(30) \quad D(t) = (NF_p + F_g + \frac{NA_R}{A_4} F_{fp}) \operatorname{sgn}(\dot{x}) + \frac{NA_R A_N}{A_4} P_N$$

$$+ NA_1\, g(v_1) + N(A_1 + A_2)\, g(v_2) + NA_R\, g(v_3)$$

From the preceding analysis

$$(5) \quad v_1 = \frac{A_1}{a_1} \dot{x}$$

$$(6) \quad v_2 = \frac{A_1 + A_2}{a_2} \dot{x}$$

$$(7) \quad v_3 = \frac{NA_R}{a_3} \dot{x}$$

$$(1) \qquad g(v_1) = \frac{\sigma}{2g}\left(\frac{v_1}{c_1}\right)^2 \operatorname{sgn}(v_1)$$

After using the moment-area equations (following section) to define the required control function [D(t)], Equation 26 is solved numerically for "x" and "$\dot{x}$" at any time "t". This allows evaluation of the function $g(v_1)$ from

$$(31) \qquad g(v_1) = \frac{1}{NA_1}\left[D(t) - \left(NF_p + F_g + \frac{NA_R}{A_4} F_{fp}\right) \operatorname{sgn}(\dot{x}) - \frac{NA_R A_N}{A_4} P_N - N(A_1 + A_2)\, g(v_2) - NA_R\, g(v_3)\right]$$

The required control orifice area is next computed from

$$(32) \qquad v_1 = \left(c_1\sqrt{\frac{2g}{\sigma}\, g(v_1)\, \operatorname{sgn}[g(v_1)]}\right) \operatorname{sgn}[g(v_1)]$$

and

$$(33) \qquad a_1 = \frac{A_1\, \dot{x}}{v_1}$$

For a quadrant elevation of zero degrees, the equation by which motion after firing is defined is (Equation 17 with B(t) = 0 and sin γ = 0)

$$(34) \qquad M_{eff}\, \ddot{x} = -\left(NF_p + F_g + \frac{NA_R}{A_4} F_{fp}\right) \operatorname{sgn}(\dot{x}) - \frac{NA_R A_N}{A_4} P_N - NA_1\, g(v_1) - N(A_1 + A_2)\, g(v_2) - NA_R\, g(v_3)$$

with "$\dot{x} < 0$" (during counterrecoil), this may be written (after assuming $c_1 \approx c_2 \approx c_3 = c$) as

$$(35) \quad M_{eff}\ddot{x} = (NF_p + F_g + \frac{NA_R}{A_4} F_{fp}) - \frac{NA_R A_N}{A_4} P_N + \frac{\sigma}{2gc^2}\left[\frac{NA_1^{\,3}}{a_1^{\,2}} + \frac{N(A_1 + A_2)^3}{a_2^{\,2}} + \frac{(NA_R)^3}{a_3^{\,2}}\right]\dot{x}^2$$

As indicated in this equation, the gas pressure "P_N" produces the negative acceleration while effective friction and hydraulic throttling produce the positive accelerations. The velocity of the recoiling parts will be constant if the acceleration is equal to zero. That is, if the following relation holds

$$(36) \quad \frac{\sigma}{2gc^2}\left[\frac{NA_1^{\,3}}{a_1^{\,2}} + \frac{N(A_1 + A_2)^3}{a_2^{\,2}} + \frac{(NA_R)^3}{a_{3af}^{\,2}}\right]\dot{x}^2 + (NF_p + F_g + \frac{NA_R}{A_4} F_{fp}) = \frac{NA_R A_N}{A_4} P_N$$

To ensure control, the friction forces can be neglected and, by proper sizing of the orifice areas (a_i), any one orifice can be made to limit the counterrecoil velocity. A specified value for the minimum counterrecoil velocity, ($\dot{x}_{min}$) can be used to define a value for "a_{3af}" through the following relation.

$$(37) \quad \frac{(NA_R)^3}{a_{3af}^{\,2}} = \left(\frac{2gc^2}{\sigma \dot{x}_{min}^{\,2}}\right)\left(\frac{NA_R A_N}{A_4} P_N\right) - \frac{N(A_1 + A_2)^3}{a_2^{\,2}} - \frac{NA_1^{\,3}}{a_1^{\,2}}$$

To limit the terminal counterrecoil velocity ($\dot{x}_T$), the value of "a_1" can be defined by the relation

$$(38) \quad \frac{NA_1^{\,3}}{a_1^{\,2}} = \frac{2gc^2}{\sigma \dot{x}_T^{\,2}}\left(\frac{NA_R A_N}{A_4} P_N\right) - \frac{N(A_1 + A_2)^3}{a_2^{\,2}} - \frac{(NA_R)^3}{a_{3af}^{\,2}}$$

Actually, the minimum value for a_1 is determined by the necessary clearance between the spear buffer and the recoil piston head. Then, at latch position,

$$a_1 = a_{1eak}$$

and, by neglecting terms that include

$$a_2 \quad \text{and} \quad a_{3af}$$

$$\text{(39)} \qquad \dot{x}_T = \sqrt{\left(\frac{2gc^2}{\sigma}\right)\left(\frac{a^2_{1eak}}{NA_1^{\,3}}\right)\left(\frac{NA_R A_N}{A_4} P_N\right)}$$

DEFINITION OF RECOIL AND COUNTERRECOIL CONTROL FUNCTIONS

Linear motion (x) of the recoiling mass (M_{eff}) is defined by a differential equation having the form:

(40) $M_{eff}\ \ddot{x} = A(t) - D(t)$

where (Figure 7):

A(t) = Summation of forces causing positive acceleration

D(t) = Summation of forces causing negative acceleration and both may be considered as functions of time.

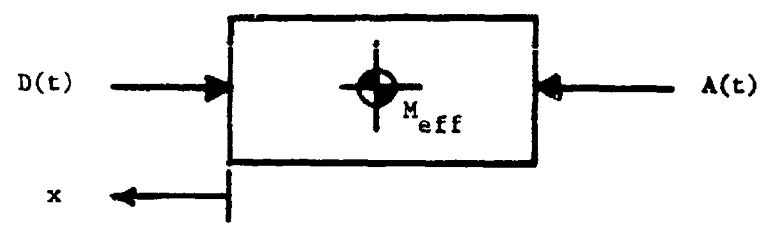

FIGURE 7

Free Body Diagram of Recoiling Mass

Since the firing cycle begins with the recoiling parts at rest, the initial conditions are:

$x = 0$ and $\dot{x} = 0$ when $t = 0$

If a definition of A(t) and D(t) is assumed, a graphical interpretation of Equation 40 at any instant ($t = t_i$) is given by the following equations. (Reference 8, Pages 6 and 7).

Moment Area Equations

$$(41)\quad M_{eff}\, \dot{x}_{t = t_i} = \int_0^{t_i} A(t)\, dt - \int_0^{t_i} D(t)\, dt$$

$$(42)\quad M_{eff}\, x_{t = t_i} = \left[t_i - \overline{A}(t)\right] \int_0^{t_i} A(t)\, dt$$

$$- \left[t_i - \overline{D}(t)\right] \int_0^{t_i} D(t)\, dt$$

where

$$(43)\quad \int_0^{t_i} A(t)\, dt = \text{Area under curve of } A(t) \text{ from } t = 0 \text{ to } t = t_i$$

$$(44)\quad \int_0^{t_i} D(t)\, dt = \text{Area under curve of } D(t) \text{ from } t = 0 \text{ to } t = t_i$$

$$(45)\quad \left[t_i - \overline{A}(t)\right] \int_0^{t_i} A(t)\, dt = \text{Moment of area under } A(t) \text{ around } t = t_i$$

$$(46)\quad \left[t_i - \overline{D}(t)\right] \int_0^{t_i} D(t)\, dt = \text{Moment of area under } D(t) \text{ around } t = t_i$$

If A(t) is prescribed forcing function (i.e., a breech force plus an effective weight component), D(t) will be a control function by which some specified motion of the mass M_{eff} is produced. Equations 41 and 42 can be used to obtain the required definition of the control function D(t).

For a conventional recoil cycle, the breech force [B(t)] is applied at t = 0 and recoil displacement must be limited. Then, let

D_o = Value of D(t) at beginning of recoil (t = 0)

D_e = Value of D(t) at end of recoil ($t = t_r$)

ℓ = Allowable recoil displacement ($x = \ell$ at $t = t_r$)

I = Area under B(t) (Impulse)

$\bar{\bar{a}}$ = Location of centroid of area under B(t)

W_{eff} = Effective weight component

A minimum peak value for D(t) can be obtained if the function is held constant over the complete recoil stroke. However, since an instantaneous increase in D(t) is impossible, a reasonable rise and fall time must be allowed. Let

Δ_r = Specified rise and fall time for D(t)

D_r = Constant level of decelerating force

The assumed force system is illustrated graphically in Figure 8.

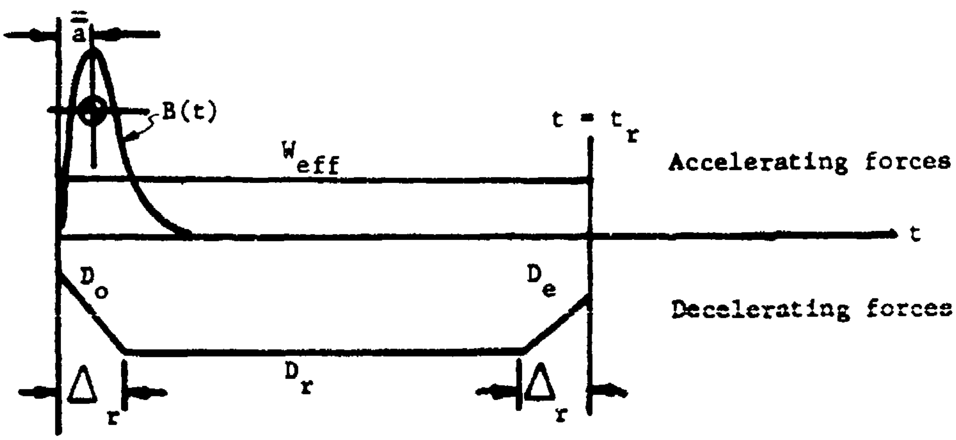

FIGURE 8

Assumed Force System for a Conventional Recoil Cycle

Equations 41 and 42 may be solved simultaneously for values of the unknowns D_R and t_R.

$$(47) \qquad t_r = \frac{4\left[M_{eff}\,\ell + I\bar{\bar{a}} + \frac{D_e - D_o}{6}\,\Delta_r^{\,2}\right]}{2I + (D_e - D_o)\,\Delta_r}$$

$$(48) \qquad D_r = \frac{I + W_{eff}\,t_r - .5\,(D_o + D_e)\,\Delta_r}{t_r - \Delta_r}$$

This defines the control function used to design the spear buffer which protects the system from damage if a maximum impulse charge is fired from latch (i.e., cook-off).

For an ideal soft-recoil cycle, the assumed force system is that shown in Figure 9.

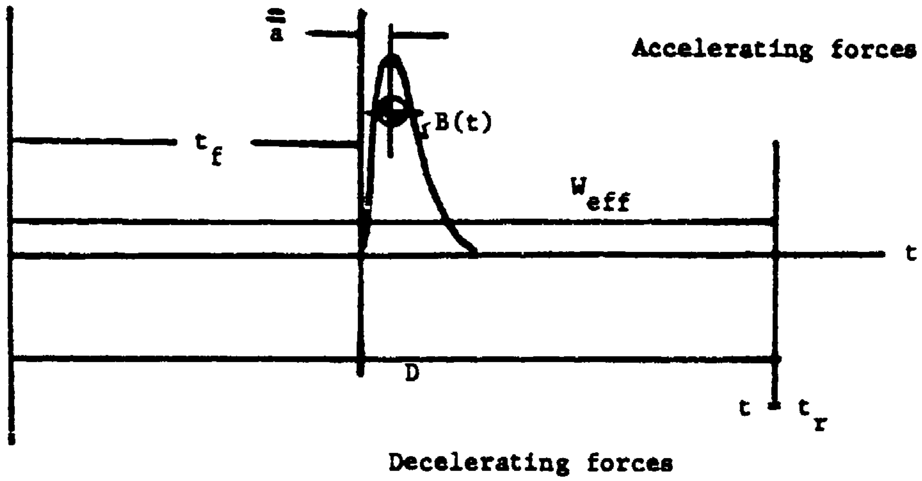

FIGURE 9

Assumed Force System for an Ideal Soft Recoil Cycle with

$$A(t) = B(t) + W_{eff}$$

$$D(t) = D \qquad \text{(Assumed constant)}$$

$$x = 0 \text{ and } \dot{x} = 0 \text{ at } t = 0 \qquad \text{(Battery)}$$

$$x = 0 \text{ and } \dot{x} = 0 \text{ at } t = t_R \qquad \text{(Return to battery)}$$

$$x = \ell \text{ and } \dot{x} = x_f \text{ at } t = t_f \qquad \text{(Firing)}$$

The moment area equations (Equations 41 and 42) can be solved for

D ——— Required drive force

t_r ——— Cycle time

$\dot{x}_f$ ——— Firing velocity

as

$$(49) \qquad D = \frac{I^2}{4(2M_{eff}\,\ell + \bar{s}I)} + W_{eff}$$

$$(50) \qquad t_r = \frac{I}{D - W_{eff}}$$

$$(51) \qquad \dot{x}_f = \frac{I}{2M_{eff}} + \frac{\bar{s}\,(D - W_{eff})}{M_{eff}}$$

During a normal soft-recoil cycle, the recoiling parts are

(1) driven forward by expansion of the gas in the recuperator;

(2) returned to a point slightly to the rear of latch position by application of the breech force; and

(3) returned to latch by the gas force.

During a maximum overload cycle (caused by firing from the latch position, the recoiling parts are

(1) driven fearward by application of the breech force;

(2) brought to a stop by hydraulic throttling of oil between the spear buffer and the recoil piston, and,

(3) returned to battery (latch position) by expansion of the compressed gas in the recuperator.

In both cases, counterrecoil control must be provided to prevent impact against the latch mechanism.

For the soft-recoil mechanism (shown schematically in Figure 2), the minimum counterrecoil velocity is limited by restriction of the fluid flow from the recuperator through the orifice area a_3. (After firing, $a_3 = a_{3af}$ as defined by Equation 37 when "$\dot{x} < 0$.") To protect the latch mechanism, final counterrecoil control is produced by use of the spear buffer to restrict the oil flow between P_2 and P_1. Use of the spear buffer for both recoil and counterrecoil control is made possible by the check valve which is effective while "$x_v > x > 0$." During recoil, $P_1 > P_2$ and the valve is opened to allow flow through the valve orifice (a_v) as well as around the spear buffer ($a_x + a_{leak}$). During counterrecoil, with $P_2 > P_1$ and the valve closed, flow between P_2 and P_1 is restricted to the annular orifice around the spear buffer ($a_x + a_{leak}$). (See Page 18).

For an acceptable counterrecoil control function, the counterrecoil velocity must be changed from $\dot{x}_{min}$ at $x = x_v$ to $\dot{x}_T$ at $x = x_T$ by throttling of fluid flow between P_2 and P_1. As a result of the restricted flow between the recuperator and recoil cylinders through the orifice a_{3af} (thereby limiting the magnitude of $\dot{x}_{min}$), the accelerating force is approximately zero when control of fluid flow through a_1 is initiated. Since the terminal velocity is to be held constant from $x = x_T$ to $x = 0$, the accelerating force will again to zero when $x = x_T$.

By substituting Equations 2, 3, and 4 in Equation 17, we obtain the following equation defining counterrecoil motion at 0° Q.E. [i.e., $B(t) = 0$, $\dot{x} < 0$ and $\sin \gamma = 0$]

$$(52) \quad \left[M_R + \left(\frac{A_4 - NA_R}{A_4}\right)^2 M_p\right] \ddot{x} = (NF_p + F_g + \frac{NA_R}{A_4} F_{fp})$$

$$- \frac{NA_R A_N}{A_4} P_N - NA_1(P_1 - P_2)$$

$$- N(A_1 + A_2)(P_2 - P_3) - NA_R(P_3 - P_4)$$

with the significant pressure drop across the orifice a_1.

$$P_N \approx P_4 \approx P_3 \approx P_2$$

and the above equation becomes

$$(53) \quad \left[M_R + \left(\frac{A_4 - NA_R}{A_4}\right)^2 M_p\right] \ddot{x} = (NF_p + F_g + \frac{NA_R}{A_4} F_{fp})$$

$$- \frac{NA_R A_N}{A_4} P_N - NA_1(P_1 - P_N)$$

If $P_1 = 0$, the accelerating force is given by

$$D = (NF_p + F_g \frac{NA_R}{A_4} F_{fp})$$

$$- \frac{NA_R A_N}{A_4} P_N + NA_1 P_N$$

$$D = (NF_p + F_g + \frac{NA_R}{A_4} F_{fp})$$

$$+ N(A_1 - \frac{A_R A_N}{A_4}) P_N$$

With counterrecoil control occurring near the latch position where $P_N \approx P_o$, a limiting design value for "D" is given by

$$(54) \qquad D = (NF_p + F_g + \frac{NA_R}{A_4} F_{fp}) + N(A_1 - \frac{A_R A_N}{A_4}) P_o$$

Based on the preceding analysis, the counterrecoil control function must satisfy the following constraints

$$D(t) = 0 \text{ when } x = x_v \text{ and } \dot{x} = \dot{x}_{min}$$

$$D(t) \leq D \text{ for } x_v < x < 0$$

$$D(t) = 0 \text{ when } x = x_T \text{ and } \dot{x} = \dot{x}_T$$

The shape of the control function may be chosen in some essentially arbitrary fashion so long as adequate flow control can be maintained. One such choice is shown (Figure 10).

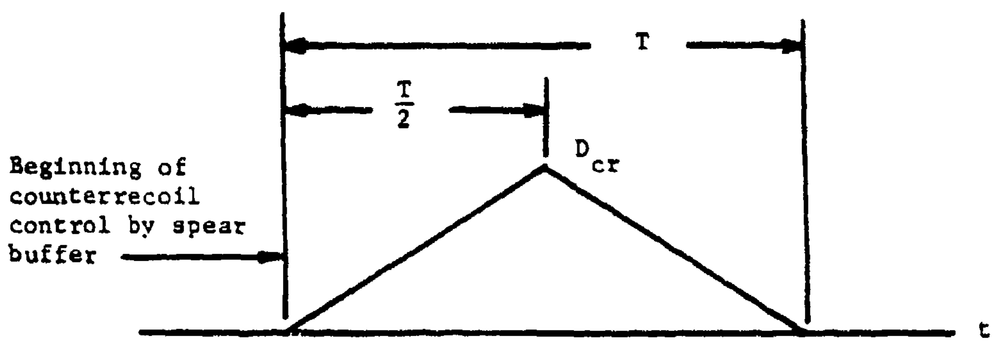

FIGURE 10

Counterrecoil Control Function

Then, from "$t = 0$ to $t = \frac{T}{2}$", motion is defined by

$$M_{eff}\ \ddot{x} = \frac{2D_{CR}}{T} \quad t$$

where

$$M_{eff} = \left[M_R + \left(\frac{A_4 - NA_R}{A_4} \right)^2 \quad M_p \right]$$

$$D_{CR} \leq (NF_p + F_g + \frac{NA_R}{A_4} \quad F_{fp}) + N(A_1 - \frac{A_R A_N}{A_4}) \quad P_o$$

NOTE: 't' is assumed zero when counterrecoil control begins.

Then,

$$M_{eff}\ \dot{x} = \frac{2D_{CR}}{T} \quad \frac{t^2}{2} \quad + \quad K_1$$

$$M_{eff}\ x = \frac{D_{CR}}{T} \quad \frac{t^3}{3} \quad + K_1\ t + K_2$$

Since

$$x = x_v \quad \text{and} \quad \dot{x} = \dot{x}_{min} \quad \text{at} \quad t = 0$$

The constants of integration are

$$K_1 = M_{eff}\ \dot{x}_{min}$$

$$K_2 = M_{eff}\ x_v$$

Therefore, at $t = \frac{T}{2}$, $\dot{x} = \dot{X}$ and $x = X$

$$M_E \dot{X} = \frac{D_{CR}}{T} \frac{T^2}{4} + M_{eff} \dot{x}_{min}$$

$$\dot{X} = \frac{D_{CR} T}{4 M_{eff}} + \dot{x}_{min}$$

and

$$M_{eff} X = \frac{D_{CR}}{3T} \frac{T^3}{8} + M_{eff} \dot{x}_{min} \frac{T}{2} + M_{eff} x_v$$

$$X = \frac{D_{CR} T^2}{24 M_{eff}} + \frac{\dot{x}_{min} T}{2} + x_v$$

While the function $D(t)$ is decreasing, the equation of motion may be written as

$$M_{eff} \ddot{x} = D_{CR} - \frac{2 D_{CR}}{T} t$$

with

$$\dot{x} = \dot{X} \text{ and } x = X \text{ at } t = 0$$

NOTE: Here, "t" has been assumed zero when the control function begins to decrease.

$$M_{eff} \dot{x} = D_{CR} t - \frac{2D_{CR}}{T} \frac{t^2}{2} + K_1$$

$$M_{eff} x = D_{CR} \frac{t^2}{2} - \frac{D_{CR}}{T} \frac{t^3}{3} + K_1 t + K_2$$

and the constants of integration are

$$K_1 = M_{eff} \dot{X}$$

$$K_2 = M_{eff} X$$

As originally specified, when "D" returns to zero

$$\dot{x} = \dot{x}_T \text{ and } x = x_T$$

Then, at $t = \frac{T}{2}$,

$$M_{eff}\,\dot{x}_T = D_{CR}\,\frac{T}{2} - \frac{D_{CR}}{T}\,\frac{T^2}{4}$$

$$+ M_{eff}\,\frac{D_{CR}\,T}{4M_{eff}} + M_{eff}\,\dot{x}_{min}$$

$$M_{eff}\,\dot{x}_T = \frac{D_{CR}\,T}{2} + M_{eff}\,\dot{x}_{min}$$

$$(55)\quad \dot{x}_{min} = \dot{x}_T - \frac{D_{CR}\,T}{2M_{eff}}$$

$$M_{eff}\,x_T = \frac{D_{CR}}{2}\,\frac{T^2}{4} - \frac{D_{CR}}{3T}\,\frac{T^3}{8}$$

$$+ \frac{D_{CR}\,T}{4}\,\frac{T}{2} + M_{eff}\,\dot{x}_{min}\,\frac{T}{2}$$

$$+ \frac{D_{CR}\,T^2}{24} + M_{eff}\,\dot{x}_{min}\,\frac{T}{2} + M_{eff}\,x_v$$

$$M_{eff}\,x_T = D_{CR}T^2\left[\frac{1}{8} - \frac{1}{24} + \frac{1}{8} + \frac{1}{24}\right]$$

$$+ M_{eff}\,\dot{x}_{min}\,T + M_{eff}\,x_v$$

$$(56) \qquad M_{eff}\, x_T = \frac{D_{CR}\, T^2}{4} + M_{eff}\, \dot{x}_{min}\, T + M_{eff}\, x_v$$

Equations 55 and 56 may be solved simultaneously for values of "T" and "x_{min}" when values for "D_{CR}, M_{eff}, $\dot{x}_T$, and x_v" are specified. By substituting Equation 55 in Equation 56,

$$M_{eff}\, x_T = \frac{D_{CR}\, T^2}{4} + M_{eff}\, T \left[\dot{x}_T - \frac{D_{CR}\, T}{2M_{eff}} \right] + M_{eff}\, x_v$$

$$M_{eff}\, x_T = \frac{D_{CR}\, T^2}{4} + M_{eff}\, \dot{x}_T\, T - \frac{D_{CR}\, T^2}{2} + M_{eff}\, x_v$$

$$(57) \qquad \frac{D_{CR}}{4}\, T^2 - M_{eff}\, \dot{x}_T\, T - M_{eff}\, (x_v - x_T) = 0$$

Equation 57 can then be solved for "T" and "x_{min}" determined by solving Equation 55.

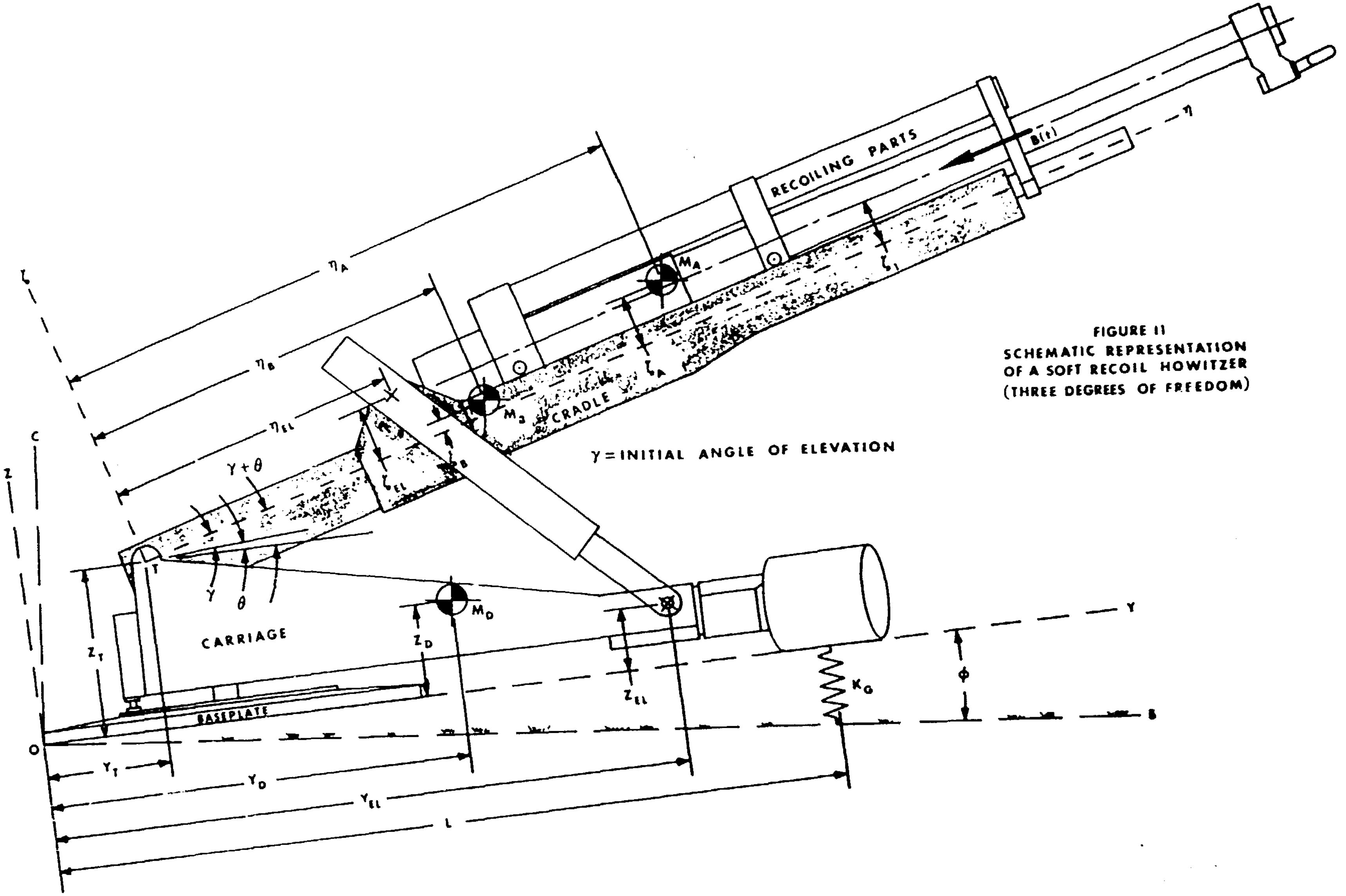

FIGURE 11
SCHEMATIC REPRESENTATION OF A SOFT RECOIL HOWITZER (THREE DEGREES OF FREEDOM)

CARRIAGE RESPONSE TO FIRING LOADS

In this model, three degrees of freedom are considered as shown in the schematic representation (Figure 11). The mass centers shown are defined as:

M_D = Mass of nonelevating portion of the weapon

M_B = Mass of elevating (but nonrecoiling) parts

M_A = Mass of recoiling parts

The three degrees of freedom may be defined in terms of the three time-dependent variables:

η_A - Defines the position of M_A with respect to the elevation trunnion

θ - Defines relative rotation between M_B and M_D around the elevation trunnion

ϕ - Defines rotation of M_D around an axis of rotation fixed in the ground

On the assumption that all motions being considered are in the plane of elevation, only planar coordinates will be required. Therefore, dimensions are defined in the positive sense according to the following coordinate systems as shown in Figure 11.

O-BC : A coordinate system fixed in the ground with its origin at the point of rotation for the mass M_D

O-YZ : A coordinate system fixed in the mass M_D (and rotating with it) having its origin at the point of rotation for this mass.

T-$\eta\zeta$: A coordinate system rotating with the mass M_B and having its origin at the elevation trunnion. At the time, t = 0, this system has been rotated through the elevation angle (γ) from its original position parallel to the O-YZ coordinate system.

From Figure 11, the following relationships may be derived:

$$Y_A = Y_T + \eta_A \cos(\gamma + \theta) - \zeta_A \sin(\gamma + \theta)$$

$$Z_A = Z_T + \eta_A \sin(\gamma + \theta) + \zeta_A \cos(\gamma + \theta)$$

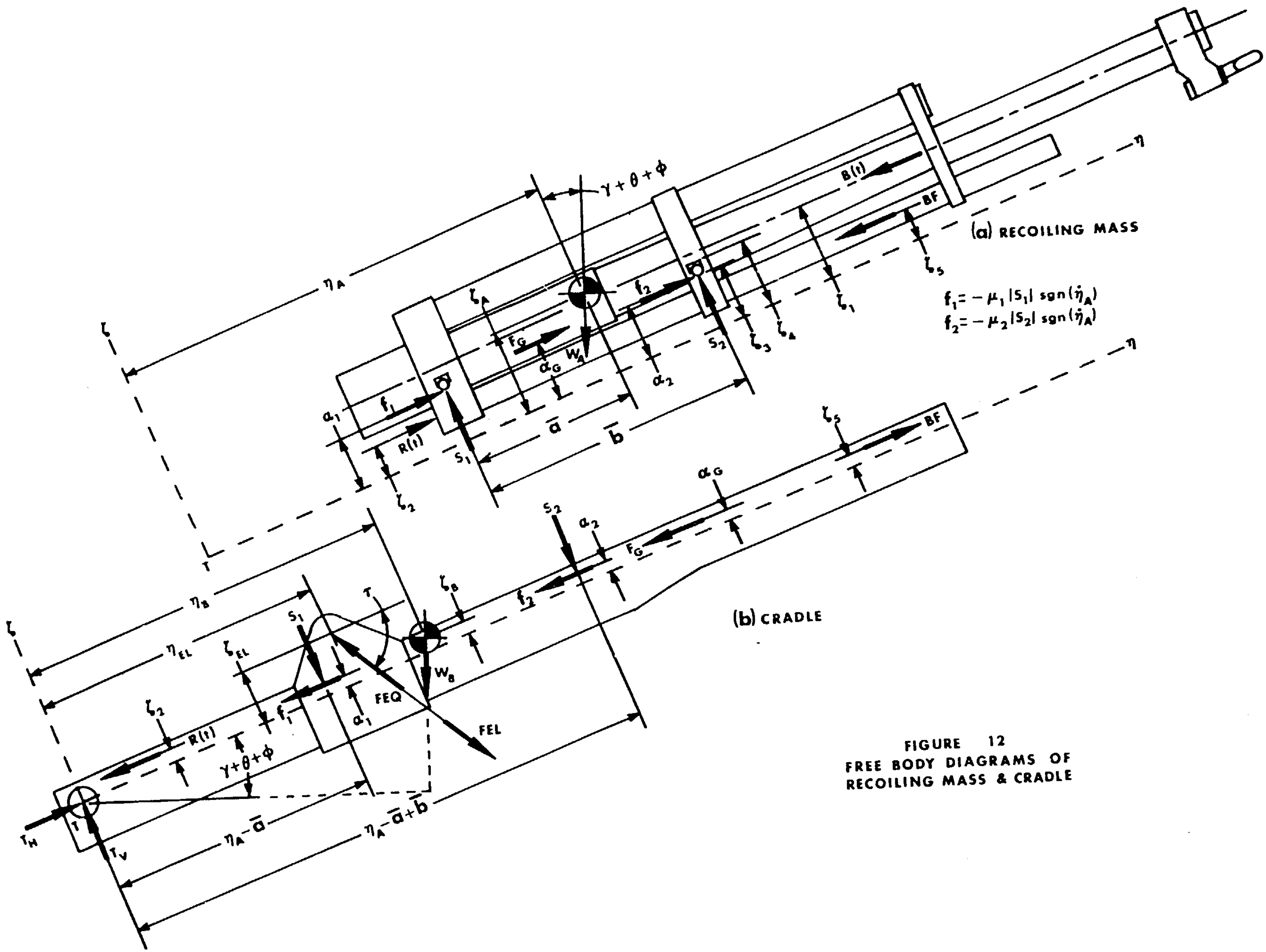

FIGURE 12
FREE BODY DIAGRAMS OF
RECOILING MASS & CRADLE

$$B_A = Y_T \cos\phi - Z_T \sin\phi + \eta_A \cos(\gamma + \theta + \phi) - \zeta_A \sin(\gamma + \theta + \phi)$$

$$C_A = Y_T \sin\phi + Z_T \cos\phi + \eta_A \sin(\gamma + \theta + \phi) + \zeta_A \cos(\gamma + \theta + \phi)$$

Similarily:

$$Y_B = Y_T + \eta_B \cos(\gamma + \theta) - \zeta_B \sin(\gamma + \theta)$$

$$Z_B = Z_T + \eta_B \sin(\gamma + \theta) + \zeta_B \cos(\gamma + \theta)$$

$$B_B = Y_T \cos\phi - Z_T \sin\phi + \eta_B \cos(\gamma + \theta + \phi) - \zeta_B \sin(\gamma + \theta + \phi)$$

$$C_B = Y_T \sin\phi + Z_T \cos\phi + \eta_B \sin(\gamma + \theta + \phi) + \zeta_B \cos(\gamma + \theta + \phi)$$

And,

$$B_D = Y_D \cos\phi - Z_T \sin\phi$$

$$C_D = Y_D \sin\phi + Z_D \cos\phi$$

Noting that η_A, θ and ϕ are time dependent variables, differentiation with respect to time gives:

$$\begin{aligned}
\dot{B}_A = &- \dot{\phi}\,[Y_T \sin\phi + Z_T \cos\phi] \\
&- (\dot{\theta} + \dot{\phi})\,[\eta_A \sin(\gamma + \theta + \phi) + \zeta_A \cos(\gamma + \theta + \phi)] \\
&+ \dot{\eta}_A \cos(\gamma + \theta + \phi)
\end{aligned}$$

$$\begin{aligned}
\dot{C}_A = &\ \dot{\phi}\,[Y_T \cos\phi - Z_T \sin\phi] \\
&+ (\dot{\theta} + \dot{\phi})\,[\eta_A \cos(\gamma + \theta + \phi) - \zeta_A \sin(\gamma + \theta + \phi)] \\
&+ \dot{\eta}_A \sin(\gamma + \theta + \phi)
\end{aligned}$$

$$\begin{aligned}
\dot{B}_B = &- \dot{\phi}\,[Y_T \sin\phi + Z_T \cos\phi] \\
&- (\dot{\theta} + \dot{\phi})\,[\eta_B \sin(\gamma + \theta + \phi) + \zeta_B \cos(\gamma + \theta + \phi)]
\end{aligned}$$

$$\begin{aligned}
\dot{C}_B = &\ \dot{\phi}\,[Y_T \cos\phi - Z_T \sin\phi] \\
&+ (\dot{\theta} + \dot{\phi})\,[\eta_B \cos(\gamma + \theta + \phi) - \zeta_B \sin(\gamma + \theta + \phi)]
\end{aligned}$$

$$\dot{B}_D = -\dot{\phi}\,[Y_D \sin\phi + Z_D \cos\phi]$$

$$\dot{C}_D = \dot{\phi}\,[Y_D \cos\phi - Z_D \sin\phi]$$

Differentiating again with respect to time gives:

$$
\begin{aligned}
\ddot{B}_A = -\ddot{\phi}\,[Y_T \sin\phi + Z_T \cos\phi] \\
&- (\ddot{\theta} + \ddot{\phi})\,[\eta_A \sin(\gamma + \theta + \phi) + \zeta_A \cos(\gamma + \theta + \phi)] \\
&+ \ddot{\eta}_A \cos(\gamma + \theta + \phi) \\
&- (\dot{\theta} + \dot{\phi})\,[2\dot{\eta}_A \sin(\gamma + \theta + \phi)] \\
&- \dot{\phi}^2\,[Y_T \cos\phi - Z_T \sin\phi] \\
&- (\dot{\theta} + \dot{\phi})^2\,[\eta_A \cos(\gamma + \theta + \phi) - \zeta_A \sin(\gamma + \theta + \phi)]
\end{aligned}
$$

$$
\begin{aligned}
\ddot{C}_A = \ddot{\phi}\,[Y_T \cos\phi - Z_T \sin\phi] \\
&+ (\ddot{\theta} + \ddot{\phi})\,[\eta_A \cos(\gamma + \theta + \phi) - \zeta_A \sin(\gamma + \theta + \phi)] \\
&+ \ddot{\eta}_A \sin(\gamma + \theta + \phi) \\
&+ (\dot{\theta} + \dot{\phi})\,[2\dot{\eta}_A \cos(\gamma + \theta + \phi)] \\
&- \dot{\phi}^2\,[Y_T \sin\phi + Z_T \cos\phi] \\
&- (\dot{\theta} + \dot{\phi})^2\,[\eta_A \sin(\gamma + \theta + \phi) + \zeta_A \cos(\gamma + \theta + \phi)]
\end{aligned}
$$

$$
\begin{aligned}
\ddot{B}_B = -\ddot{\phi}\,[Y_T \sin\phi + Z_T \cos\phi] \\
&- (\ddot{\theta} + \ddot{\phi})\,[\eta_B \sin(\gamma + \theta + \phi) + \zeta_B \cos(\gamma + \theta + \phi)] \\
&- \dot{\phi}^2\,[Y_T \cos\phi - Z_T \sin\phi] \\
&- (\dot{\theta} + \dot{\phi})^2\,[\eta_B \cos(\gamma + \theta + \phi) - \zeta_B \sin(\gamma + \theta + \phi)]
\end{aligned}
$$

$$
\begin{aligned}
\ddot{C}_B = \ddot{\phi}\,[Y_T \cos\phi + Z_T \sin\phi] \\
&+ (\ddot{\theta} + \ddot{\phi})\,[\eta_B \cos(\gamma + \theta + \phi) - \zeta_B \sin(\gamma + \theta + \phi)] \\
&- \dot{\phi}^2\,[Y_T \sin\phi + Z_T \cos\phi] \\
&- (\dot{\theta} + \dot{\phi})^2\,[\eta_B \sin(\gamma + \theta + \phi) + \zeta_B \cos(\gamma + \theta + \phi)]
\end{aligned}
$$

$$\ddot{B}_D = - \ddot{\phi}\,[Y_D \sin\phi + Z_D \cos\phi] - \dot{\phi}^2\,[Y_D \cos\phi - Z_D \sin\phi]$$

$$\ddot{C}_D = \ddot{\phi}\,[Y_D \cos\phi - Z_D \sin\phi] - \dot{\phi}^2\,[Y_D \sin\phi + Z_D \cos\phi]$$

By defining

T = Kinetic energy of the system

V = Potential energy of the system

F_ϕ, F_θ = Generalized forces (torques) causing rotations ϕ and θ

the Lagrange equations become:

For pitch motion (defined by ϕ):

$$\text{(58)} \quad \frac{d}{dt}\left[\frac{\partial T}{\partial \dot{\phi}}\right] - \frac{\partial T}{\partial \phi} + \frac{\partial V}{\partial \phi} = F_\phi$$

For relative rotation (defined by θ):

$$\text{(59)} \quad \frac{d}{dt}\left[\frac{\partial T}{\partial \dot{\theta}}\right] - \frac{\partial T}{\partial \theta} + \frac{\partial V}{\partial \theta} = F_\theta$$

If I_A, I_B and I_D are mass moments of inertia of each mass around its mass center, the kinetic energy may be defined in terms of velocity components (referenced to the fixed coordinate system O-BC) and rotational velocities as:

$$T = \frac{1}{2} M_A [\dot{B}_A^2 + \dot{C}_A^2] + \frac{1}{2} M_B [\dot{B}_B^2 + \dot{C}_B^2] + \frac{1}{2} M_D [\dot{B}_D^2 + \dot{C}_D^2] + \frac{1}{2} [I_A + I_B] [\dot{\theta} + \dot{\phi}]^2 + \frac{1}{2} I_D \dot{\phi}^2$$

After terms are expanded and collected, the following expression for kinetic energy is obtained:

$$
\begin{aligned}
(60)\quad T = \frac{M_A}{2}\Bigg[\, & \dot{\phi}^2\,[Y_T^2 + Z_T^2 + \eta_A^2 + \zeta_A^2 + 2(\eta_A Y_T + \zeta_A Z_T)\cos(\gamma + \theta) \\
& \qquad + 2(\eta_A Z_T - \zeta_A Y_T)\sin(\gamma + \theta)] \\
& + \dot{\theta}^2[\eta_A^2 + \zeta_A^2] + \dot{\eta}_A^2 \\
& + 2\dot{\phi}\dot{\theta}\,[\eta_A^2 + \zeta_A^2 + (\eta_A Y_T + \zeta_A Z_T)\cos(\gamma + \theta) \\
& \qquad + (\eta_A Z_T - \zeta_A Y_T)\sin(\gamma + \theta)] \\
& - 2\zeta_A\dot{\theta}\,\dot{\eta}_A - 2\dot{\eta}_A\dot{\phi}\,[\zeta_A - Y_T\sin(\gamma + \theta) + Z_T\cos(\gamma + \theta)]\,\Bigg] \\
+ \frac{M_B}{2}\Bigg[\, & \dot{\phi}^2\,[Y_T^2 + Z_T^2 + \eta_B^2 + \zeta_B^2 + 2(\eta_B Y_T + \zeta_B Z_T)\cos(\gamma + \theta) \\
& \qquad + 2(\eta_B Z_T - \zeta_B Y_T)\sin(\gamma + \theta)] \\
& + \dot{\theta}^2[\eta_B^2 + \zeta_B^2] \\
& + 2\dot{\phi}\dot{\theta}\,[\eta_B^2 + \zeta_B^2 + (\eta_B Y_T + \zeta_B Z_T)\cos(\gamma + \theta) \\
& \qquad + (\eta_B Z_T - \zeta_B Y_T)\sin(\gamma + \theta)]\,\Bigg] \\
& + \frac{M_D}{2}\dot{\phi}^2[Y_D^2 + Z_D^2] + \frac{I_A + I_B}{2}[\dot{\phi} + \dot{\theta}]^2 + \frac{I_D}{2}\dot{\phi}^2
\end{aligned}
$$

Differentiating Equation 60 with respect to $\dot{\phi}$:

$$\frac{\partial T}{\partial \dot{\phi}} = M_A \Big[\dot{\phi} \, [Y_T^{\,2} + Z_T^{\,2} + \eta_A^{\,2} + \zeta_A^{\,2} + 2(\eta_A Y_T + \zeta_A Z_T) \cos (\gamma + \theta)$$

$$+ 2(\eta_A Z_T - \zeta_A Y_T) \sin (\gamma + \theta)]$$

$$+ \dot{\theta} \, [\eta_A^{\,2} + \zeta_A^{\,2} + (\eta_A Y_T + \zeta_A Z_T) \cos (\gamma + \theta)$$

$$+ (\eta_A Z_T - \zeta_A Y_T) \sin (\gamma + \theta)]$$

$$- \dot{\eta}_A \, [\zeta_A - Y_T \sin (\gamma + \theta) + Z_T \cos (\gamma + \theta)] \Big]$$

$$+ M_B \Big[\dot{\phi} \, [Y_T^{\,2} + Z_T^{\,2} + \eta_B^{\,2} + \zeta_B^{\,2} + 2(\eta_B Y_T + \zeta_B Z_T) \cos (\gamma + \theta)$$

$$+ 2(\eta_B Z_T - \zeta_B Y_T) \sin (\gamma + \theta)]$$

$$+ \dot{\theta} \, [\eta_B^{\,2} + \zeta_B^{\,2} + (\eta_B Y_T + \zeta_B Z_T) \cos (\gamma + \theta)$$

$$+ (\eta_B Z_T - \zeta_B Y_T) \sin (\gamma + \theta)] \Big]$$

$$+ M_D \, \dot{\phi} [Y_D^{\,2} + Z_D^{\,2}] + [I_A + I_B] [\dot{\phi} + \dot{\theta}] + I_D \, \dot{\phi}$$

And then with respect to time

$$(61)\quad \frac{d}{dt}\left[\frac{\partial T}{\partial \dot\phi}\right] = \ddot\phi\Big[M_A\,[Y_T^2 + Z_T^2 + \eta_A^2 + \zeta_A^2 + 2(\eta_A Y_T + \zeta_A Z_T)\cos(\gamma+\theta)$$

$$+ 2(\eta_A Z_T - \zeta_A Y_T)\sin(\gamma+\theta)]$$

$$+ M_B\,[Y_T^2 + Z_T^2 + \eta_B^2 + \zeta_B^2 + 2(\eta_B Y_T + \zeta_B Z_T)\cos(\gamma+\theta)$$

$$+ 2(\eta_B Z_T - \zeta_B Y_T)\sin(\gamma+\theta)]$$

$$M_D\,[Y_D^2 + Z_D^2] + [I_A + I_B + I_D]\Big]$$

$$+ \ddot\theta\Big[M_A\,[\eta_A^2 + \zeta_A^2 + (\eta_A Y_T + \zeta_A Z_T)\cos(\gamma+\theta)$$

$$+ (\eta_A Z_T - \zeta_A Y_T)\sin(\gamma+\theta)]$$

$$+ M_B\,[\eta_B^2 + \zeta_B^2 + (\eta_B Y_T + \zeta_B Z_T)\cos(\gamma+\theta)$$

$$+ (\eta_B Z_T - \zeta_B Y_T) - \sin(\gamma+\theta)]$$

$$+ [I_A + I_B]\Big]$$

$$-\ddot\eta_A M_A\,[\zeta_A - Y_T\sin(\gamma+\theta) + Z_T\cos(\gamma+\theta)]$$

$$- 2\dot\phi\dot\theta\Big[M_A[(\eta_A Y_T + \zeta_A Z_T)\sin(\gamma+\theta) - (\eta_A Z_T - \zeta_A Y_T)\cos(\gamma+\theta)]$$

$$+ M_B\,[\eta_B Y_T + \zeta_B Z_T)\sin(\gamma+\theta) - (\eta_B Z_T - \zeta_B Y_T)\cos(\gamma+\theta)]\Big]$$

$$+ 2\dot\theta\,\dot\eta_A M_A\,[\eta_A + Y_T\cos(\gamma+\theta) + Z_T\sin(\gamma+\theta)]$$

$$+ 2\,\dot\eta_A\dot\phi\, M_A\,[\eta_A + Y_T\cos(\gamma+\theta) + Z_T\sin(\gamma+\theta)]$$

$$- \dot\theta^2\Big[M_A\,[\eta_A Y_T + \zeta_A Z_T)\sin(\gamma+\theta) - (\eta_A Z_T - \zeta_A Y_T)\cos(\gamma+\theta)]$$

$$+ M_B\,[\eta_B Y_T + \zeta_B Z_T)\sin(\gamma+\theta) - (\eta_B Z_T - \zeta_B Y_T)\cos(\gamma+\theta)]\Big]$$

Similarily, differentiating Equation 60 first with respect to $\dot{\theta}$

$$\frac{\partial T}{\partial \dot{\theta}} = M_A \Big[\dot{\theta} \, [\eta_A^2 + \zeta_A^2]$$

$$+ \dot{\phi} \, [\eta_A^2 + \zeta_A^2 + (\eta_A Y_T + \zeta_A Z_T) \cos(\gamma + \theta) + (\eta_A Z_T - \zeta_A Y_T) \sin(\gamma + \theta)]$$

$$- \zeta_A \dot{\eta}_A \Big]$$

$$+ M_B \Big[\dot{\theta} \, [\eta_B^2 + \zeta_B^2]$$

$$+ \dot{\phi} \, [\eta_B^2 + \zeta_B^2 + (\eta_B Y_T + \zeta_B Z_T) \cos(\gamma + \theta) + (\eta_B Z_T - \zeta_B Y_T) \sin(\gamma + \theta)] \Big]$$

$$+ [I_A + I_B] \, [\dot{\phi} + \dot{\theta}]$$

And then with respect to time,

$$(62) \quad \frac{d}{dT} \left[\frac{\partial T}{\partial \dot{\theta}} \right] = \ddot{\phi} \Big[M_A \, [\eta_A^2 + \zeta_A^2 + (\eta_A Y_T + \zeta_A Z_T) \cos(\gamma + \theta)$$

$$+ (\eta_A Z_T - \zeta_A Y_T) \sin(\gamma + \theta)]$$

$$+ M_B \, [\eta_B^2 + \zeta_B^2 + (\eta_B Y_T + \zeta_B Z_T) \cos(\gamma + \theta)$$

$$+ (\eta_B Z_T - \zeta_B Y_T) \sin(\gamma + \theta)]$$

$$+ [I_A + I_B] \Big]$$

$$+ \ddot{\theta} \Big[M_A \, [\eta_A^2 + \zeta_A^2] + M_B \, [\eta_B^2 + \zeta_B^2] + [I_A + I_B] \Big] + \ddot{\eta}_A \, [-M_A \zeta_A]$$

$$- \dot{\phi}\dot{\theta} \Big[M_A \, [(\eta_A Y_T + \zeta_A Z_T) \sin(\gamma + \theta) - (\eta_A Z_T - \zeta_A Y_T) \cos(\gamma + \theta)]$$

$$+ M_B \, [(\eta_B Y_T + \zeta_B Z_T) \sin(\gamma + \theta) - (\eta_B Z_T - \zeta_B Y_T) \cos(\gamma + \theta)] \Big]$$

$$+ \dot{\theta}\dot{\eta}_A \, [2 M_A \eta_A] + \dot{\eta}_A \dot{\phi} \, M_A \, [2\eta_A + Y_T \cos(\gamma + \theta) + Z_T \sin(\gamma + \theta)]$$

Next, differentiating Equation 60 with respect to ϕ

$$(63) \quad \frac{\partial T}{\partial \phi} = 0$$

and with respect to θ

$$(64) \quad \frac{\partial T}{\partial \theta} = - \dot{\phi}\dot{\theta}\Big[M_A\ [(\eta_A Y_T + \zeta_A Z_T) \sin(\gamma + \theta) - (\eta_A Z_T - \zeta_A Y_T) \cos(\gamma + \theta)]$$

$$+ M_B\ [(\eta_B Y_T + \zeta_B Z_T) \sin(\gamma + \theta) - (\eta_B Z_T - \zeta_B Y_T) \cos(\gamma + \theta)]\Big]$$

$$+ \dot{\theta}\dot{\eta}_A\ [0]$$

$$+ \dot{\eta}_A\ \dot{\phi}\ M_A\ [Y_T \cos(\gamma + \theta) + Z_T \sin(\gamma + \theta)]$$

$$- \dot{\phi}^2\Big[M_A\ [(\eta_A Y_T + \zeta_A Z_T) \sin(\gamma + \theta) - (\eta_A Z_T - \zeta_A Y_T) \cos(\gamma + \theta)]$$

$$+ M_B\ [(\eta_B Y_T + \zeta_B Z_T) \sin(\gamma + \theta) - (\eta_B Z_T - \zeta_B Y_T) \cos(\gamma + \theta)]\Big]$$

The potential energy in the system may be defined as the sum of

V_W = Potential energy due to weight

V_G = Potential energy stored in the effective spring at the front support point.

V_{EQ} = Potential energy stored in the equilibrators

V_{EL} = Potential energy stored in the elevation struts

That is,

$$(65) \quad V = V_W + V_G + V_{EQ} + V_{EL}$$

Since the change in potential energy with respect to each of the generalized coordinates is the important factor in the Lagrange equation, any reference position may be used. This analysis is based on the following definition for the reference position:

$$\eta_A = \eta_{AO}$$

$$\phi = 0$$

$$\theta = 0$$

The potential energy due to weight is given by:

$$V_W = C_A W_A + C_B W_B + C_D W_D$$

or

$$V_W = [Y_T \sin \phi + Z_T \cos \phi + \eta_A \sin (\gamma + \theta + \phi) + \zeta_A \cos (\gamma + \theta + \phi)] W_A$$
$$+ [Y_T \sin \phi + Z_T \cos \phi + \eta_B \sin (\gamma + \theta + \phi) + \zeta_B \cos (\gamma + \theta + \phi)] W_B$$
$$+ [Y_D \sin \phi + Z_D \cos \phi] W_D \tag{66}$$

Then, differentiating Equation 66 with respect to ϕ and with respect to θ,

$$\frac{\partial V_W}{\partial \phi} = [Y_T \cos \phi - Z_T \sin \phi + \eta_A \cos (\gamma + \theta + \phi) - \zeta_A \sin (\gamma + \theta + \phi)] W_A$$
$$+ [Y_T \cos \phi - Z_T \sin \phi + \eta_B \cos (\gamma + \theta + \phi) - \zeta_B \sin (\gamma + \theta + \phi)] W_B$$
$$+ [Y_D \cos \phi - Z_D \sin \phi] W_D \tag{67}$$

$$\frac{\partial V_W}{\partial \theta} = [\eta_A \cos (\gamma + \theta + \phi) - \zeta_A \sin (\gamma + \theta + \phi)] W_A$$
$$+ [\eta_B \cos (\gamma + \theta + \phi) - \zeta_B \sin (\gamma + \theta + \phi)] W_B \tag{68}$$

By defining static equilibrium as the reference position, the static load in the ground spring is given by

$$P_{static} = \frac{B_A W_A + B_B W_B + B_D W_D}{L}$$

and, if we assume an effective spring having a linear load-deflection relationship with

$$K_G = \text{Effective Spring Rate}$$

a static deflection of the spring can be defined as:

$$\Delta_{G static} = P_{static} / K_G$$

The deflection of the spring due to the pitch motion ϕ is given by

$$\Delta_{G\phi} = - L \phi$$

The minus sign decreases the spring deflection as ϕ increases when $L > 0$ (i.e. - when the pivot point is at the rear), and increases the spring deflection as ϕ increases when $L < 0$ (i.e. - when the pivot point is in front of the spring). This allows the total spring deflection to be written as:

$$\Delta_G = \Delta_{G\phi} + \Delta_{G_{static}}$$

Then, the potential energy in this spring is given by:

$$V_G = \frac{1}{2} (K_G \Delta_G) \Delta_G = \frac{1}{2} K_G \Delta_G^2$$

$$V_G = \frac{1}{2} K_G [\Delta_{G\phi} + \Delta_{G_{static}}]^2$$

$$= \frac{1}{2} K_G \left[- L \phi + \frac{P_{static}}{K_G}\right]^2$$

$$= \frac{1}{2} K_G \left[- L\left(\phi - \frac{P_{static}}{K_G L}\right)\right]^2$$

$$= \frac{K_G L^2}{2}\left[\phi - \frac{P_{static}}{K_G L}\right]^2$$

Letting

$$\phi_{static} = \frac{P_{static}}{K_G L}$$

or

$$\phi_{static} = \frac{B_A W_A + B_B W_B + B_D W_D}{K_G L^2}$$

The potential energy can be written as

$$(69) \quad V_G = \frac{1}{2} K_G L^2 (\phi - \phi_{static})^2$$

Then, differentiating with respect to ϕ and θ gives

$$(70) \quad \frac{\partial V_G}{\partial \phi} = K_G L^2 (\phi - \phi_{static})$$

and

$$(71) \quad \frac{\partial V_G}{\partial \theta} = 0$$

The equilibrators and elevating struts will act as co-linear spring elements whose potential energies change with their change in length. To establish this change in length, the following coordinates may be defined:

$$Y_1 = Y_T + \eta_{EL} \cos (\gamma + \theta) - \zeta_{EL} \sin (\gamma + \theta)$$

$$Z_1 = Z_T + \eta_{EL} \sin (\gamma + \theta) + \zeta_{EL} \cos (\gamma + \theta)$$

$$Y_2 = Y_{EL}$$

$$Z_2 = Z_{EL}$$

Then, the length of the elevating struts is given by:

$$LEL_{\gamma + \theta} = [(Y_1 - Y_2)^2 + (Z_1 - Z_2)^2]^{1/2}$$

Substitution, expansion, and collection of terms allows the writing of:

$$LEL_{\gamma + \theta} = \Big[(Y_T - Y_{EL})^2 + (Z_T - Z_{EL})^2 + \eta_{EL}^2 + \zeta_{EL}^2$$

$$+ 2[(Y_T - Y_{EL})\, \eta_{EL} + (Z_T - Z_{EL})\, \zeta_{EL}] \cos (\gamma + \theta)$$

$$- 2[(Y_T - Y_{EL})\, \zeta_{EL} - (Z_T - Z_{EL})\, \eta_{EL}] \sin (\gamma + \theta)\Big]^{1/2}$$

By defining the constants:

$$(72)\quad EL1 = (Y_T - Y_{EL})^2 + (Z_T - Z_{EL})^2 + \eta_{EL}{}^2 + \zeta_{EL}{}^2$$

$$(73)\quad EL2 = [(Y_T - Y_{EL})\ \eta_{EL} + (Z_T - Z_{EL})\ \zeta_{EL}]$$

$$(74)\quad EL3 = [(Y_T - Y_{EL})\ \zeta_{EL} - (Z_T - Z_{EL})\ \eta_{EL}]$$

The length may be written as

$$(75)\quad LEL_{\gamma + \theta} = [EL1 + 2EL2 \cos (\gamma + \theta) - 2EL3 \sin (\gamma + \theta)]^{1/2}$$

A spring equilibrator (compression type) is shown schematically in Figure 13.

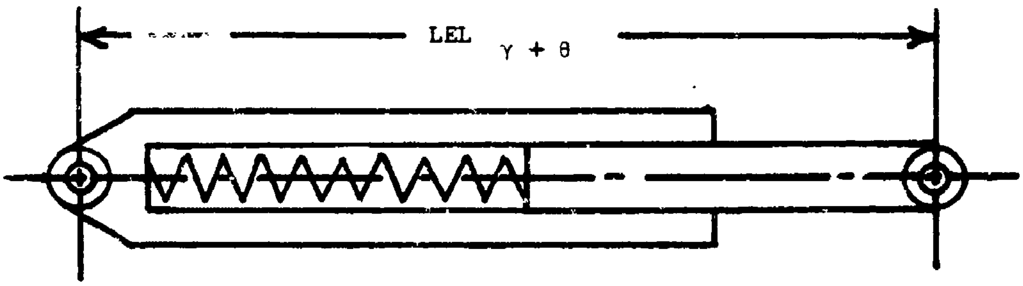

FIGURE 13

Spring Equilibrator - Compression Type

Let

PEQ = Preload in equilibrator spring (i.e. - load at $\gamma = 0°$)

K_{EQ} = Spring rate of equilibrator spring

Then, the total force for two parallel equilibrators is given by

$$FEQ_{\gamma+\theta} = 2\,[PEQ - K_{EQ}\,(LEL_{\gamma+\theta} - LEL_0)] \tag{76}$$

With the reference position defined by $\theta = 0$, the potential energy stored in the equilibrator is given by

$$V_{EQ} = \int_{LEL_\gamma}^{LEL_{\gamma+\theta}} FEQ_{\gamma+\theta}\; d\,(LEL_{\gamma+\theta})$$

$$= \int_{LEL_\gamma}^{LEL_{\gamma+\theta}} 2[PEQ - K_{EQ}\,(LEL_{\gamma+\theta} - LEL_0)]\; d\,(LEL_{\gamma+\theta})$$

$$= 2\int_{LEL_\gamma}^{LEL_{\gamma+\theta}} [PEQ + K_{EQ}\,LEL_0 - K_{EQ}\,(LEL_{\gamma+\theta})]\,d\,(LEL_{\gamma+\theta})$$

$$= 2\left[(PEQ + K_{EQ}\,LEL_0)\,(LEL_{\gamma+\theta}) - K_{EQ}\,\frac{LEL_{\gamma+\theta}}{2}\right]_{LEL_\gamma}^{LEL_{\gamma+\theta}}$$

$$= 2\left[(PEQ + K_{EQ}\,LEL_0)\,(LEL_{\gamma+\theta} - LEL_\gamma)\right.$$

$$\left. - \frac{K_{EQ}}{2}\,(LEL_{\gamma+\theta}^{\;2} - LEL_\gamma^{\;2})\right]$$

Then

$$\frac{\partial V_{EQ}}{\partial\theta} = 2\left[(PEQ + K_{EQ}\,LEL_0)\,\frac{\partial LEL_{\gamma+\theta}}{\partial\theta}\right.$$

$$\left. - K_{EQ}\,LEL_{\gamma+\theta}\,\frac{\partial LEL_{\gamma+\theta}}{\partial\theta}\right]$$

$$(77) \quad \frac{\partial V_{EQ}}{\partial \theta} = 2\,[F_{EQ} - K_{EQ}\,(LEL_{\gamma+\theta} - LEL_0)]\,\frac{\partial LEL_{\gamma+\theta}}{\partial \theta}$$

and, since V_{EQ} is indpendent of the variable ϕ

$$(78) \quad \frac{\partial V_{EQ}}{\partial \phi} = 0$$

The elevation struts contain preloaded ring spring assemblies as shown in Figure 14.

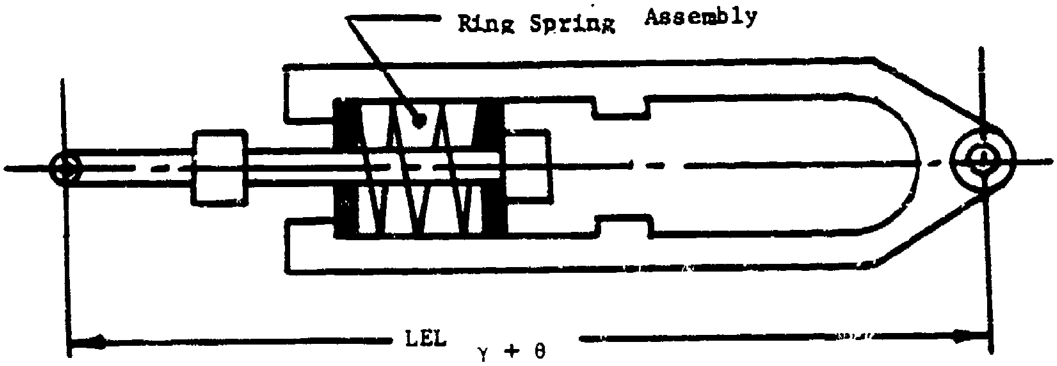

FIGURE 14
Schematic Diagram of Elevation Strut

Treating an increase in length as a positive deflection of the spring assembly and defining a tension load as positive enables one to depict graphically the force in one strut (Figure 15).

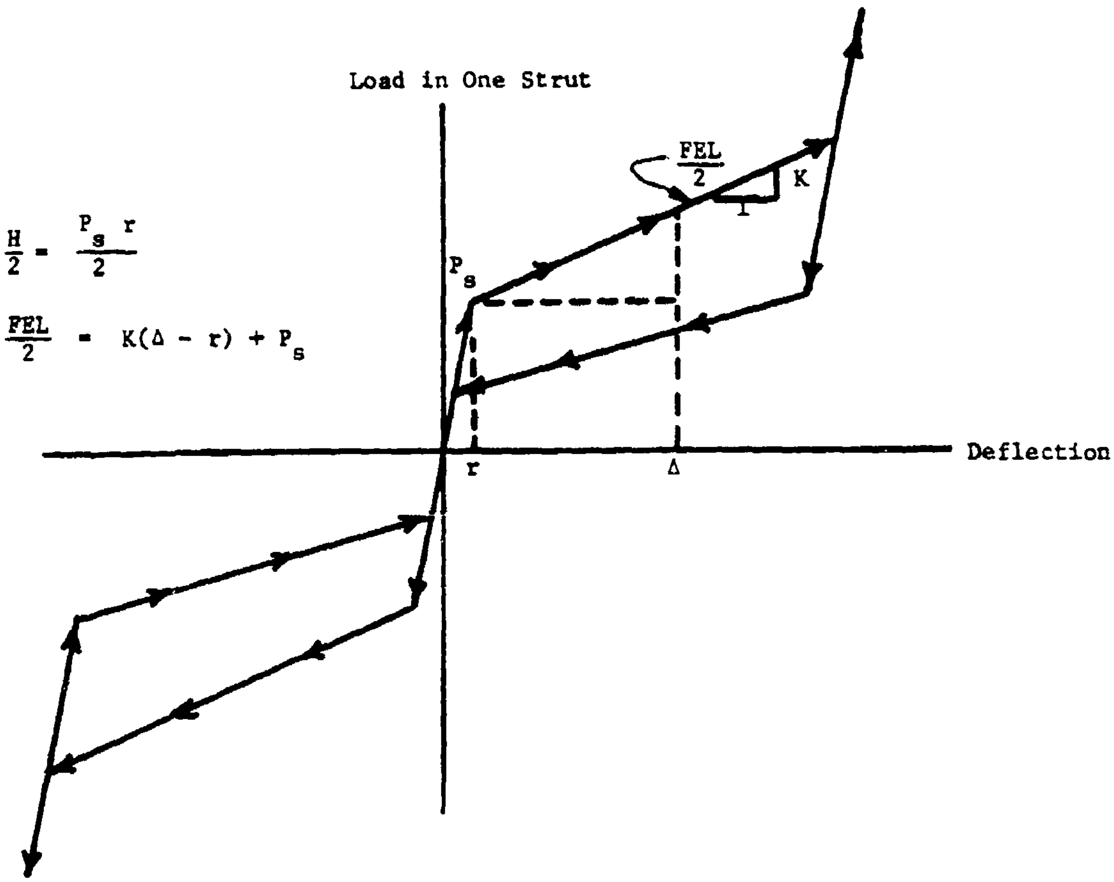

FIGURE 15
Load Deflection Curve for one Elevation Strut

Note that the value of FEL is taken as zero at time 0. Then the spring deflection is given by

$$\Delta = LEL_{\gamma + \theta} - LEL_{\gamma}$$

Since the load in the elevation strut must be defined in a piecewise fashion, the potential energy will also be defined in this manner. With the equilibrators approximately balancing the tipping parts when $\theta = 0$, the potential energy in the elevation struts (both) may be defined as twice the area between the load deflection curve and the Δ axis from $\Delta = 0$ to Δ. The curve chosen will be dependent on whether the spring assembly is being compressed or releasing its energy.

The potential energy (V_{EL}) can be expressed as a function of the strut deflection Δ in the form

$$(79) \qquad V_{EL} = [\Delta - r]^2 K + 2[\Delta - r] P_s + H$$

where the constants r, K, P_s and H are defined in a piecewise fashion. (See Figure 15).

Since Δ is independent of ϕ

$$(80) \qquad \frac{\partial V_{EL}}{\partial \phi} = 0$$

However,

$$\frac{\partial V_{EL}}{\partial \theta} = 2 [\Delta - r] K \frac{\partial \Delta}{\partial \theta} + 2P_s \frac{\partial \Delta}{\partial \theta}$$

$$= 2 \left[K [\Delta - r] + P_s \right] \frac{\partial \Delta}{\partial \theta}$$

and since

$$\Delta = LEL_{\gamma + \theta} - LEL_{\gamma}$$

The equation

$$(81) \qquad \frac{\partial V_{EL}}{\partial \theta} = 2 \left[K [LEL_{\gamma + \theta} - LEL_{\gamma} - r] + P_s \right] \frac{\partial LEL_{\gamma + \theta}}{\partial \theta}$$

is obtained

Recalling that (Equation 65)

$$V = V_W + V_G + V_{EQ} + V_{EL}$$

The following relations may be written

$$\frac{\partial V}{\partial \phi} = \frac{\partial V_W}{\partial \phi} + \frac{\partial V_G}{\partial \phi} + \frac{\partial V_{EQ}}{\partial \phi} + \frac{\partial V_{EL}}{\partial \phi}$$

$$\frac{\partial V}{\partial \theta} = \frac{\partial V_W}{\partial \theta} + \frac{\partial V_G}{\partial \theta} + \frac{\partial V_{EQ}}{\partial \theta} + \frac{\partial V_{EL}}{\partial \theta}$$

Then, making the appropriate substitutions in the above equations, using Equations 67, 70, 78 and 80

$$\begin{aligned}(82)\quad \frac{\partial V}{\partial \phi} = {} & [Y_T \cos \phi - Z_T \sin \phi + \eta_A \cos (\gamma + \theta + \phi) - \zeta_A \sin (\gamma + \theta + \phi)]\ W_A \\ & + [Y_T \cos \phi - Z_T \sin \phi + \eta_B \cos (\gamma + \theta + \phi) - \zeta_B \sin (\gamma + \theta + \phi)]\ W_B \\ & + [Y_D \cos \phi - Z_D \sin \phi]\ W_D + K_G\ L^2(\phi - \phi_{static})\end{aligned}$$

Using Equations 68, 71, 77, and 81

$$\begin{aligned}\frac{\partial V}{\partial \theta} = {} & [\eta_A \cos (\gamma + \theta + \phi) - \zeta_A \sin (\gamma + \theta + \phi)]\ W_A \\ & + [\eta_B \cos (\gamma + \theta + \phi) - \zeta_B \sin (\gamma + \theta + \phi)]\ W_B \\ & + 2\ [PEQ - K_{EQ}\ (LEL_{\gamma + \theta} - LEL_{\gamma})]\ \frac{\partial LEL_{\gamma + \theta}}{\partial \theta} \\ & + 2[K(LEL_{\gamma + \theta} - LEL_{\gamma} - r) + P_s]\ \frac{\partial LEL_{\gamma + \theta}}{\partial \theta}\end{aligned}$$

which may be written

$$(83)\quad \frac{\partial V}{\partial \theta} = [\eta_A \cos(\gamma + \theta + \phi) - \zeta_A \sin(\gamma + \theta + \phi)]\, W_A$$

$$+ [\eta_B \cos(\gamma + \theta + \phi) - \zeta_B \sin(\gamma + \theta + \phi)]\, W_B$$

$$- 2 \left[K_{EQ} \left(\begin{array}{c} [EL1 + 2EL2 \cos(\gamma + \theta) - 2EL3 \sin(\gamma + \theta)]^{1/2} \\ - [EL1 + 2EL2]^{1/2} \end{array} \right) - P_{EQ} \right]$$

$$\left[\frac{EL2 \sin(\gamma + \theta) + EL3 \cos(\gamma + \theta)}{[EL1 + 2EL2 \cos(\gamma + \theta) - 2EL3 \sin(\gamma + \theta)]^{1/2}} \right]$$

$$-2 \left[K \left(\begin{array}{c} [EL1 + 2EL2 \cos(\gamma + \theta) - 2EL3 \sin(\gamma + \theta)]^{1/2} \\ - [EL1 + 2EL2 \cos\gamma - 2EL3 \sin\gamma]^{1/2} - r \end{array} \right) + P_s \right]$$

$$\left[\frac{EL2 \sin(\gamma + \theta) + EL3 \cos(\gamma + \theta)}{[EL1 + 2EL2 \cos(\gamma + \theta) - 2EL3 \sin(\gamma + \theta)]^{1/2}} \right]$$

By the resolution of the breech force [B(t)] into a force along the η - axis and a couple around the point T and by including the dissipation functions representing damping in the ground spring and in the elevation trunnion, the generalized forces may be taken as the torques around the appropriate pivot points (O and T). Then,

$$F_{\phi} = B(t)\,\zeta_1 - Y_T\,B(t)\sin(\gamma + \theta) + Z_T\,B(t)\cos(\gamma + \theta) - c_{\phi}\,\dot{\phi}$$

$$F_{\phi} = B(t)\,\zeta_1 - c_{\theta}\,\dot{\theta}$$

or

(84) $$F_{\phi} = [\zeta_1 - Y_T\sin(\gamma + \theta) + Z_T\cos(\gamma + \theta)]\,B(t) - c_{\phi}\,\dot{\phi}$$

(85) $$F_{\theta} = B(t)\,\zeta_1 - c_{\theta}\,\dot{\theta}$$

Then, since the Lagrange Equation for the pitch motion (defined by ϕ) is

$$\frac{d}{dt}\left[\frac{\partial T}{\partial \dot{\phi}}\right] - \frac{\partial T}{\partial \phi} + \frac{\partial V}{\partial \phi} = F_{\phi}$$

and for the relative rotation of masses M_B and M_D (defined by θ) is

$$\frac{d}{dt}\left[\frac{\partial T}{\partial \dot{\theta}}\right] - \frac{\partial T}{\partial \theta} + \frac{\partial V}{\partial \theta} = F_{\theta}$$

proper substitution enables the following equations to be written

Equation 89 (See Page 64)

Equation 90 (See Page 64)

In obtaining the equation for linear motion of the mass center, Newton's Equations may be used. From Figure 11

$$\ddot{\vec{Q}} = \ddot{B}_A \vec{j} + \ddot{C}_A \vec{k}$$

where $\ddot{B}_A$ and $\ddot{C}_A$ are components of the acceleration of the recoiling mass in the fixed coordinate system O-BC. Then the acceleration components of the recoiling mass in the η and ζ directions are

$$\ddot{Q}_\eta = \ddot{B}_A \cos(\gamma + \theta + \phi) + \ddot{C}_A \sin(\gamma + \theta + \phi)$$

$$\ddot{Q}_\zeta = -\ddot{B}_A \sin(\gamma + \theta + \phi) + \ddot{C}_A \cos(\gamma + \theta + \phi)$$

Substituting for $\ddot{B}_A$ and $\ddot{C}_A$ and simplifying gives

$$\begin{aligned}\ddot{Q}_\eta = {} & \ddot{\phi}\,[Y_T \sin(\gamma + \theta) - Z_T \cos(\gamma + \theta) - \zeta_A] \\ & - \ddot{\theta}\,\zeta_A \\ & + \ddot{\eta}_A \\ & - 2\,\dot{\phi}\dot{\theta}\,\eta_A - \dot{\theta}^2\,\eta_A - \dot{\phi}^2[\eta_A + Y_T \cos(\gamma + \theta) + Z_T \sin(\gamma + \theta)]\end{aligned}$$

and

$$\begin{aligned}\ddot{Q}_\zeta = {} & \ddot{\phi}\,[Y_T \cos(\gamma + \theta) + Z_T \sin(\gamma + \theta) + \eta_A] \\ & + \ddot{\theta}\,[\eta_A] \\ & - 2\dot{\phi}\dot{\theta}\,\zeta_A + 2\dot{\theta}\,\dot{\eta}_A + 2\,\dot{\eta}_A\,\dot{\phi} \\ & - \dot{\theta}^2\,\zeta_A - \dot{\phi}_A^{\,2}[\zeta_A - Y_T \sin(\gamma + \theta) + Z_T \cos(\gamma + \theta)]\end{aligned}$$

Now, from Figure 12(a) (page 40)

$$(86) \quad \Sigma F_\eta = M_A \ddot{Q}_\eta = R(t) - B(t) + [f_1 + f_2 + F_G] - BF - W_A \sin(\gamma + \theta + \phi)$$

$$(87) \quad \Sigma F_\zeta = M_A \ddot{Q}_\zeta = S_1 + S_2 - W_A \cos(\gamma + \theta + \phi)$$

$$(88) \quad \Sigma M_{\text{Mass Center}} = I_A (\ddot{\theta} + \ddot{\phi}) = S_2 (\bar{b} - \bar{a}) - S_1 (\bar{a}) + B(t) [\zeta_1 - \zeta_A] - BF (\zeta_A - \zeta_5) + R(t) [\zeta_A - \zeta_2] + [f_1 (\zeta_A - \alpha_1) + f_2 (\zeta_A - \alpha_2) + (\zeta_A - \alpha_G) F_G]$$

Then, the equation for linear motion of the recoiling parts is (by substituting for $\ddot{Q}_\eta$ in Equation 86)

Equation 91 (See Page 64)

Equations 89, 90, and 91 are the governing motion equations which define the variables

$$\phi, \theta \text{ and } \eta_A$$

(and their derivatives) during the firing cycle.

EQUATION 89

$$
\ddot{\phi}\left\{\begin{array}{l}
M_A[Y_T^2+Z_T^2+\eta_A^2+\zeta_A^2+2(\eta_A Y_T+\zeta_A Z_T)\cos(\gamma+\theta)+2(\eta_A Z_T-\zeta_A Y_T)\sin(\gamma+\theta)] \\
+M_B[Y_T^2+Z_T^2+\eta_B^2+\zeta_B^2+2(\eta_B Y_T+\zeta_B Z_T)\cos(\gamma+\theta)+2(\eta_B Z_T-\zeta_B Y_T)\sin(\gamma+\theta)] \\
+M_D[Y_D^2+Z_D^2]+[I_A+I_B+I_D]
\end{array}\right\}
$$

$$
+\ddot{\theta}\left\{\begin{array}{l}
M_A[\eta_A^2+\zeta_A^2+(\eta_A Y_T+\zeta_A Z_T)\cos(\gamma+\theta)+(\eta_A Z_T-\zeta_A Y_T)\sin(\gamma+\theta)] \\
+M_B[\eta_B^2+\zeta_B^2+(\eta_B Y_T+\zeta_B Z_T)\cos(\gamma+\theta)+(\eta_B Z_T-\zeta_B Y_T)\sin(\gamma+\theta)] \\
+[I_A+I_B]
\end{array}\right\}
$$

$$
+\ddot{\eta}_A\left\{-M_A[\zeta_A-Y_T\sin(\gamma+\theta)+Z_T\cos(\gamma+\theta)]\right\}=
$$

$$
[B(t)][\zeta_1-Y_T\sin(\gamma+\theta)+Z_T\cos(\gamma+\theta)]-c_\phi\dot{\phi}
$$

$$
-W_A[Y_T\cos\phi-Z_T\sin\phi+\eta_A\cos(\gamma+\theta+\phi)-\zeta_A\sin(\gamma+\theta+\phi)]
$$

$$
-W_B[Y_T\cos\phi-Z_T\sin\phi+\eta_B\cos(\gamma+\theta+\phi)-\zeta_B\sin(\gamma+\theta+\phi)]
$$

$$
-W_D[Y_D\cos\phi-Z_D\sin\phi]-K_6L^2(\phi-\phi_{static})
$$

$$
+2\dot{\phi}\dot{\theta}\left\{\begin{array}{l}
M_A[(\eta_A Y_T+\zeta_A Z_T)\sin(\gamma+\theta)-(\eta_A Z_T-\zeta_A Y_T)\cos(\gamma+\theta)] \\
+M_B[(\eta_B Y_T+\zeta_B Z_T)\sin(\gamma+\theta)-(\eta_B Z_T-\zeta_B Y_T)\cos(\gamma+\theta)]
\end{array}\right\}
$$

$$
-2\dot{\theta}\dot{\eta}_A M_A[\eta_A+Y_T\cos(\gamma+\theta)+Z_T\sin(\gamma+\theta)]
$$

$$
-2\dot{\eta}_A\dot{\phi}M_A[\eta_A+Y_T\cos(\gamma+\theta)+Z_T\sin(\gamma+\theta)]
$$

$$
+\dot{\theta}^2\left\{\begin{array}{l}
M_A[(\eta_A Y_T+\zeta_A Z_T)\sin(\gamma+\theta)-(\eta_A Z_T-\zeta_A Y_T)\cos(\gamma+\theta)] \\
+M_B[(\eta_B Y_T+\zeta_B Z_T)\sin(\gamma+\theta)-(\eta_B Z_T-\zeta_B Y_T)\cos(\gamma+\theta)]
\end{array}\right\}
$$

EQ

$$
\ddot{\phi}\left\{\begin{array}{l}
M_A[\eta_A^2+\zeta_A^2+(\eta_A Y_T+\zeta_A Z_T \\
+M_B[\eta_B^2+\zeta_B^2+(\eta_B Y_T+\zeta_B Z_T \\
+[I_A+I_B]
\end{array}\right.
$$

$$
+\ddot{\theta}\left\{M_A[\eta_A^2+\zeta_A^2]+M_B[\eta\right.
$$

$$
+\ddot{\eta}_A[-M_A\zeta_A]=
$$

$$
[B(t)]\zeta_1-c_\theta\dot{\theta}-W_A[\eta_A\cos(\gamma+\theta
$$

$$
-
$$

$$
+2\left\{K_{EQ}\left[\begin{array}{l}
[EL1+2EL2\cos(\gamma+\theta \\
-[EL1+2
\end{array}\right.\right.
$$

$$
\left\{\overline{[El}\right.
$$

$$
+2\left\{K\left[\begin{array}{l}
[EL1+2EL2\cos(\gamma+\theta) \\
-[EL1+2EL2\cos\gamma-
\end{array}\right.\right.
$$

$$
\left\{\overline{[El}\right.
$$

$$
+\dot{\phi}\dot{\theta}[0]+\dot{\theta}\dot{\eta}_A[-2M
$$

$$
-\dot{\phi}^2\left\{\begin{array}{l}
M_A[(\eta_A Y_T+ \\
+M_B[(\eta_B Y_T+
\end{array}\right.
$$

EQUATION 91

$$
\ddot{\phi}M_A[Y_T\sin(\gamma+\theta)-Z_T\cos(\gamma+\theta)-\zeta_A]+\ddot{\theta}[-M_A\zeta_A]+\ddot{\eta}_A M_A=
$$

$$
R(t)-B(t)-[\mu_1|S_1|+\mu_2|S_2|+F_G]\mathrm{sgn}(\dot{\eta}_A)-BF-W_A\sin(\gamma+\theta+\phi)+2\dot{\phi}\dot{\theta}M_A\eta_A+\dot{\theta}^2M_A\eta
$$

9

$$\gamma+\theta)+2(\eta_A Z_T-\zeta_A Y_T)\sin(\gamma+\theta)]$$
$$\gamma+\theta)+2(\eta_B Z_T-\zeta_B Y_T)\sin(\gamma+\theta)]\Big\}$$

$$\gamma+\theta)+(\eta_A Z_T-\zeta_A Y_T)\sin(\gamma+\theta)]$$
$$\gamma+\theta)+(\eta_B Z_T-\zeta_B Y_T)\sin(\gamma+\theta)]\Big\}$$

$$Z_T\cos(\gamma+\theta)]\Big\}=$$

$$\dot{\phi}$$

$$+\phi)-\zeta_A\sin(\gamma+\theta+\phi)]$$

$$\gamma+\theta+\phi)-\zeta_B\sin(\gamma+\theta+\phi)]$$

$$K_6 L^{\epsilon}(\phi-\phi_{static})$$

$$Z_T-\zeta_A Y_T)\cos(\gamma+\theta)]$$
$$Z_T-\zeta_B Y_T)\cos(\gamma+\theta)]\Big\}$$

$$_T\sin(\gamma+\theta)]$$

$$+Z_T\sin(\gamma+\theta)]$$

$$\gamma+\theta)-(\eta_A Z_T-\zeta_A Y_T)\cos(\gamma+\theta)]$$
$$\gamma+\theta)-(\eta_B Z_T-\zeta_B Y_T)\cos(\gamma+\theta)]\Big\}$$

EQUATION 90

$$\ddot{\phi}\left\{\begin{array}{l} M_A[\eta_A^2+\zeta_A^2+(\eta_A Y_T+\zeta_A Z_T)\cos(\gamma+\theta)+(\eta_A Z_T-\zeta_A Y_T)\sin(\gamma+\theta)] \\ +\ M_B[\eta_B^2+\zeta_B^2+(\eta_B Y_T+\zeta_B Z_T)\cos(\gamma+\theta)+(\eta_B Z_T-\zeta_B Y_T)\sin(\gamma+\theta)] \\ +\ [I_A+I_B] \end{array}\right\}$$

$$+\ \ddot{\theta}\left\{M_A[\eta_A^2+\zeta_A^2]+M_B[\eta_B^2+\zeta_B^2]+[I_A+I_B]\right\}$$

$$+\ \ddot{\eta}_A[-M_A\zeta_A]\ =$$

$$[B(t)]\zeta_1-c_\theta\dot{\theta}-W_A[\eta_A\cos(\gamma+\theta+\phi)-\zeta_A\sin(\gamma+\theta+\phi)]$$

$$-\ W_B[\eta_B\cos(\gamma+\theta+\phi)-\zeta_B\sin(\gamma+\theta+\phi)]$$

$$+\ 2\left\{K_{EO}\begin{bmatrix}[EL1+2EL2\cos(\gamma+\theta)-2EL3\sin(\gamma+\theta)]^{1/2} \\ -[EL1+2EL2]^{1/2}\end{bmatrix}-P_{EO}\right\}$$
$$\left\{\frac{EL2\sin(\gamma+\theta)+EL3\cos(\gamma+\theta)}{[EL1+2EL2\cos(\gamma+\theta)-2EL3\sin(\gamma+\theta)]^{1/2}}\right\}$$

$$+2\left\{K\begin{bmatrix}[EL1+2EL2\cos(\gamma+\theta)-2EL3\sin(\gamma+\theta)]^{1/2} \\ -[EL1+2EL2\cos\gamma-2EL3\sin\gamma]^{1/2}-r\end{bmatrix}+P_S\right\}$$
$$\left\{\frac{EL2\sin(\gamma+\theta)+EL3\cos(\gamma+\theta)}{[EL1+2EL2\cos(\gamma+\theta)-2EL3\sin(\gamma+\theta)]^{1/2}}\right\}$$

$$+\ \dot{\phi}\dot{\theta}[0]\ +\ \dot{\theta}\dot{\eta}_A[-2M_A\eta_A]\ +\ \dot{\eta}_A\dot{\phi}[-2M_A\eta_A]$$

$$-\ \dot{\phi}^2\left\{\begin{array}{l} M_A[(\eta_A Y_T+\zeta_A Z_T)\sin(\gamma+\theta)-(\eta_A Z_T-\zeta_A Y_T)\cos(\gamma+\theta)] \\ +M_B[(\eta_B Y_T+\zeta_B Z_T)\sin(\gamma+\theta)-(\eta_B Z_T-\zeta_B Y_T)\cos(\gamma+\theta)] \end{array}\right\}$$

EQUATION 91

$$+\ \ddot{\theta}[-M_A\zeta_A]\ +\ \ddot{\eta}_A M_A\ =$$

$$B(t)-[\mu_1|S_1|+\mu_2|S_2|+F_G]\mathrm{sgn}(\dot{\eta}_A)-BF-W_A\sin(\gamma+\theta+\phi)+2\dot{\phi}\dot{\theta}M_A\eta_A+\dot{\theta}^2M_A\eta_A+\dot{\phi}^2M_A[\eta_A+Y_T\cos(\gamma+\theta)+Z_T\sin(\gamma+\theta)]$$

2

Note that the breech force [B(t)] is the only forcing function included in Equations 89 and 90. However, the following functions are included in Equation 91:

1. R(t) - Force due to recoil mechanism

2. $-[f_1 + f_2 + F_G)\ \mathrm{sgn}\ (\dot{\eta}_A)$ - Force due to guide friction

3. BF - Force due to forward buffer

These must be defined directly or in terms of the motions which produce the forces.

Previously, the force due to the recoil mechanism [R(t)] has been defined (Equation 19) in terms of the oil pressures P_1, P_2 and P_3 (Figure 2). A comparison of the variables η_A and x leads to the following definitions

(92) $x = \eta_{Ao} - \eta_A$

(93) $\dot{x} = -\dot{\eta}_A$

(94) $\ddot{x} = -\ddot{\eta}_A$

These relations can be used to solve the equations (Table I) of fluid flow in the recoil mechanism simultaneously with the equations (Equations 89, 90, and 91) defining carriage response to firing loads.

In a similar manner, the effect of the forward buffer (required in case of a misfire) can be included. The necessary equations are derived in the Appendix.

In either Equation 17.2 or Equation 21, the guide friction was assumed to be constant and denoted by the term F_G. To be more accurate, this force is dependent on the reactions (S_1 and S_2) applied at the guide bearing points (Figure 12). That is, for the carriage response model, guide friction is

$$(f_1 + f_2 + F_G)\ \mathrm{sgn}\ (\dot{x}) = -[\mu_1|S_1| + \mu_2|S_2| + F_G]\ \mathrm{sgn}\ \dot{\eta}_A$$

The reactions S_1 and S_2 are determined in the following section.

EVALUATION OF DYNAMIC REACTIONS

In reality, this is a continuation of the carriage response model. In fact, the clip reactions (S_1 and S_2) must be determined to solve Equations 89, 90 and 91. These are evaluated as follows:

From Equation 87

$$S_1 + S_2 = W_A \cos(\gamma + \theta + \phi) + M_A \ddot{Q}_\zeta$$

or, substituting for $\ddot{Q}_\zeta$

$$\begin{aligned} S_1 + S_2 = {} & W_A \cos(\gamma + \theta + \phi) \\ & + M_A \Big[\ddot{\phi} \left[Y_T \cos(\gamma + \theta) + Z_T \sin(\gamma + \theta) + \eta_A \right] \\ & + \ddot{\theta}\, \eta_A - 2\, \dot{\phi}\dot{\theta}\, \zeta_A + 2\, \dot{\theta}\, \dot{\eta}_A + 2\, \dot{\eta}_A\, \dot{\phi} \\ & - \dot{\theta}^2 \zeta_A - \dot{\phi}^2 \left[\zeta_A - Y_T \sin(\gamma + \theta) + Z_T \cos(\gamma + \theta) \right] \Big] \end{aligned}$$

From Equation 88

$$\begin{aligned} S_1 (\bar{a}) - S_2 (\bar{b} - \bar{a}) = {} & B(t) \left[\zeta_1 - \zeta_A \right] - BF (\zeta_A - \zeta_5) \\ & + R(t) \left[\zeta_A - \zeta_2 \right] \\ & + \left[f_1 (\zeta_A - \alpha_1) + f_2 (\zeta_A - \alpha_2) + (\zeta_A - \alpha_G) F_G \right] \\ & - I_A (\ddot{\theta} + \ddot{\phi}) \end{aligned}$$

Let

(95) $\quad \text{RAIL} = -[\mu_1|S_1|(\zeta_A - \alpha_1) + \mu_2|S_2|(\zeta_A - \alpha_2) + (\zeta_A - \alpha_G) F_G] \operatorname{sgn}(\dot{\eta}_A)$

(96) $\quad \text{XYZ1} = B(t)\ [\zeta_1 - \zeta_A] - BF\ (\zeta_A - \zeta_5)$

$$+ R(t)\ [\zeta_A - \zeta_2] - I_A\ (\ddot{\theta} + \ddot{\phi})$$

(97) $$\text{XYZ} = M_A \left\{ \begin{array}{l} \ddot{\phi}\ [Y_T \cos(\gamma + \theta) + Z_T \sin(\gamma + \theta) + \eta_A] \\ + \ddot{\theta}\eta_A - 2\dot{\phi}\dot{\theta}\zeta_A + 2\dot{\theta}\dot{\eta}_A + 2\dot{\eta}_A\dot{\phi} - \dot{\theta}^2\ \zeta_A \\ - \dot{\phi}^2[\zeta_A - Y_T \sin(\gamma + \theta) + Z_T \cos(\gamma + \theta)] \end{array} \right\} + W_A \cos(\gamma + \theta + \phi)$$

Then,

$$S_1 + S_2 = \text{XYZ}$$

$$S_1(\bar{a}) - S_2\ (\bar{b} - \bar{a}) = \text{XYZ1} + \text{RAIL}$$

Solving simultaneously,

(98) $$S_2 = \frac{\text{XYZ}\ (\bar{a}) - \text{XYZ1} - \text{RAIL}}{\bar{b}}$$

(99) $$S_1 = \text{XYZ} - S_2$$

These may be solved for S_1 and S_2 by a simple iterative scheme after assuming starting values and continuing until the solution converges.

The force in the two equilibrators has been defined as (page 55)

$$(76)\quad FEQ_{\gamma+\theta} = 2[PEQ - KEQ\ (LEL_{\gamma+\theta} - LEL_{U})]$$

and the force in the two elevation struts is given by (See Figure 15)

$$FEL_{\gamma+\theta} = 2[(\Delta - r)\ K + P_s]$$

or

$$(100)\quad FEL_{\gamma+\theta} = 2[(LEL_{\gamma+\theta} - LEL_{\gamma} - r)\ K + P_s]$$

where (page 53)

$$(75)\quad LEL_{\gamma+\theta} = [EL1 + 2EL2\ \cos\ (\gamma + \theta) - 2EL3\ \sin\ (\gamma + \theta)]^{1/2}$$

In evaluating the trunnion reactions, the components of acceleration for the mass M_B are:

in the η direction,

$$\ddot{R}_{\eta} = \ddot{B}_{B}\ \cos\ (\gamma + \theta + \phi) + \ddot{C}_{P}\ \sin\ (\gamma + \theta + \phi)$$

and in the ζ direction,

$$\ddot{R}_{\zeta} = -\ddot{B}_{B}\ \sin\ (\gamma + \theta + \phi) + \ddot{C}_{B}\ \cos\ (\gamma + \theta + \phi)$$

Substituting for $\ddot{B}_B$ and $\ddot{C}_B$ and simplifying allows writing these components in the following form

$$\ddot{R}_\eta = - \ddot{\phi} [\zeta_B - Y_T \sin (\gamma + \theta) + Z_T \cos (\gamma + \theta)] - \ddot{\theta}\zeta_B - 2\dot{\phi}\dot{\theta}\eta_B$$

$$- \dot{\phi}^2 [\eta_B + Y_T \cos (\gamma + \theta) + Z_T \sin (\gamma + \theta)] - \dot{\theta}^2 \eta_B$$

and

$$\ddot{R}_\zeta = \ddot{\phi} [\eta_B + Y_T \cos (\gamma + \theta) + Z_T \sin (\gamma + \theta)] + \ddot{\theta}\eta_B - 2\dot{\phi}\dot{\theta}\zeta_B$$

$$- \dot{\phi}^2 [\zeta_B - Y_T \sin (\gamma + \theta) + Z_T \cos (\gamma + \theta)] - \dot{\theta}^2 \zeta_B$$

Then, from the free body diagram of the cradle [Figure 12(b)]

$$\Sigma F_\eta = M_B\ddot{R}_\eta = T_H - FEQ_{\gamma + \theta} \cos \tau - R(t) + BF$$

$$+ FEL_{\gamma + \theta} \cos \tau - W_B \sin (\gamma + \theta + \phi)$$

$$+ \{f_1 + f_2 + F_G\}$$

and

$$\Sigma F_\zeta = M_B\ddot{R}_\zeta = T_V + FEQ_{\gamma + \theta} \sin \tau - S_1 - S_2$$

$$- FEL_{\gamma + \theta} \sin \tau - W_B \cos (\gamma + \theta + \phi)$$

where (Figure 12)

$$\tau = \tan^{-1} \frac{Z_1 - Z_{EL}}{Y_{EL} - Y_1} + (\gamma + \theta)$$

NOTE: The angle τ will be in the first or second quadrant

(101) $$\tau = \tan^{-1} \frac{Z_T + \eta_{EL} \sin(\gamma + \theta) + \zeta_{EL} \cos(\gamma + \theta) - Z_{EL}}{Y_{EL} - Y_T - \eta_{EL} \cos(\gamma + \theta) + \zeta_{EL} \sin(\gamma + \theta)} + (\gamma + \theta)$$

Then,

(102) $$T_H = - M_B \Big[\ddot{\phi} \left[\zeta_B - Y_T \sin(\gamma + \theta) + Z_T \cos(\gamma + \theta) \right] + \ddot{\theta} \zeta_B + 2\dot{\phi}\dot{\theta}\eta_B$$

$$+ \dot{\phi}^2 \left[\eta_B + Y_T \cos(\gamma + \theta) + Z_T \sin(\gamma + \theta) \right] + \dot{\theta}^2 \eta_B \Big]$$

$$+ FEQ_{\gamma + \theta} \cos\tau + R(t) - [\mu_1 |S_1| + \mu_2 |S_2| + F_G] \operatorname{sgn}(\dot{\eta}_A)$$

$$- BF - FEL_{\gamma + \theta} \cos\tau + W_B \sin(\gamma + \theta + \phi)$$

And

(103) $$T_V = M_B \Big[\ddot{\phi} [\eta_B + Y_T \cos(\gamma + \theta) + Z_T \sin(\gamma + \theta)] + \ddot{\theta} \eta_B - 2\dot{\phi}\dot{\theta}\zeta_B$$

$$- \dot{\phi}^2 [\zeta_B - Y_T \sin(\gamma + \theta) + Z_T \cos(\gamma + \theta)] - \dot{\theta}^2 \zeta_B \Big]$$

$$- FEQ_{\gamma + \theta} \sin\tau + S_1 + S_2 + FEL_{\gamma + \theta} \sin\tau + W_B \cos(\gamma + \theta + \phi)$$

The free body diagram of the mass M_D is shown in Figure 16. Since this mass is also assumed to simply rotate around point 0, the constants,

$$(104) \qquad \bar{\beta} = \left| \tan^{-1} \frac{Z_D}{Y_D} \right|$$

and

$$(105) \qquad R_D = [Y_D^2 + Z_D^2]^{1/2}$$

may be used in evaluating the reactions at the support points. As defined on Page 50, the total spring deflection is given by

$$\Delta_G = \Delta_{G\phi} + \Delta_{G_{static}}$$

Then, since

$$\Delta_{G\phi} = -L\phi$$

and

$$\Delta G_{static} = \frac{P_{static}}{K_G}$$

$$(106) \qquad \phi_{static} = \frac{P_{static}}{K_G L}$$

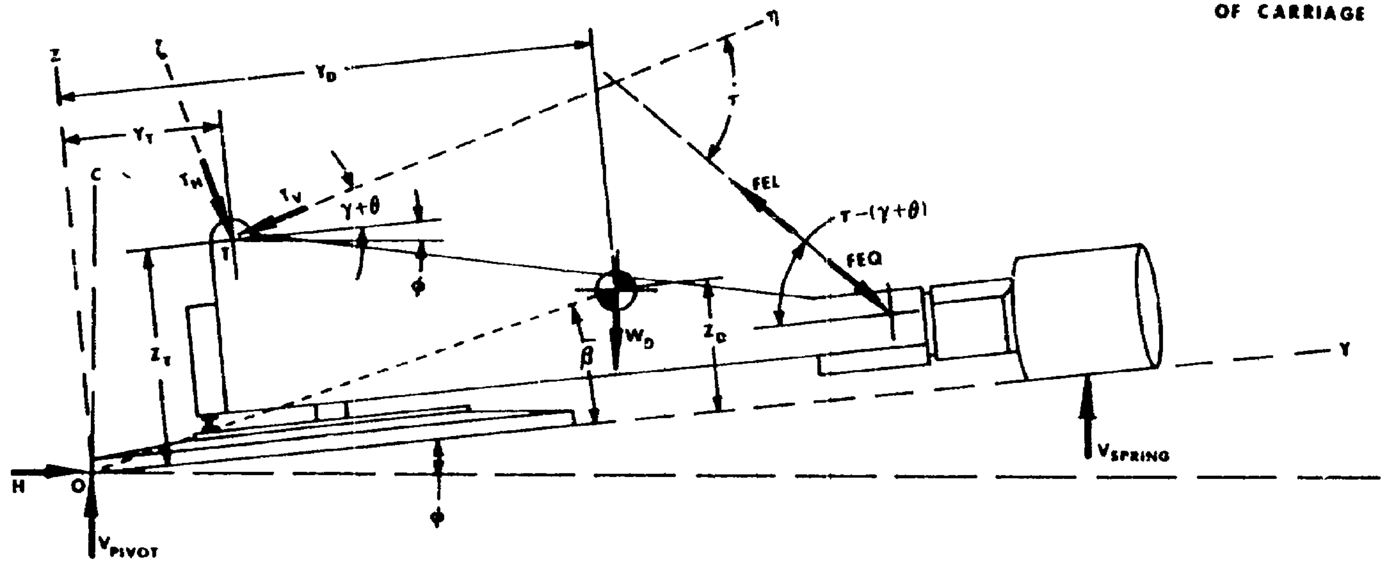

FIGURE 16
FREE BODY DIAGRAM
OF CARRIAGE (M_D)

where P_{static} may be evaluated as (Page 50)

$$P_{static} = \frac{B_A + W_A + B_B W_B + B_D W_D}{L}$$

Therefore,

$$\Delta_G = - L (\phi - \phi_{static})$$

The reaction at the effective spring is given by

$$V_{spring} = K_G \Delta_G$$

(107) $$V_{spring} = - K_G L (\phi - \phi_{static})$$

From the free body diagram of the Mass M_D (Figure 16)

$$\Sigma F_B = M_D [R_D \ddot{\phi}] \sin (\bar{\beta} + \phi) =$$

$$T_H \cos (\gamma + \theta + \phi) - T_V \sin (\gamma + \theta + \phi)$$

$$+ \; FEL_{\gamma + \theta} \cos (\tau - \gamma - \theta - \phi)$$

$$- \; FEQ_{\gamma + \theta} \cos (\tau - \gamma - \theta - \phi) - H$$

$$\Sigma F_C = M_D \, [R_D \ddot{\phi}] \cos (\bar{\beta} + \phi) =$$

$$V_{spring} + FEL_{\gamma + \theta} \sin (\tau - \gamma - \theta - \phi)$$

$$- T_H \sin (\gamma + \theta + \phi) - T_V \cos (\gamma + \theta + \phi)$$

$$- FEQ_{\gamma + \theta} \sin (\tau - \gamma - \theta - \phi)$$

$$- W_D + V_{pivot}$$

Therefore,

$$(108) \quad V_{pivot} = T_H \sin (\gamma + \theta + \phi) + T_V \cos (\gamma + \theta + \phi)$$

$$- FEL_{\gamma + \theta} \sin (\tau - \gamma - \theta - \phi)$$

$$+ FEQ_{\gamma + \theta} \sin (\tau - \gamma - \theta - \phi) + W_D - V_{spring}$$

$$+ [M_D \, R_D \cos (\bar{\beta} + \phi)] \, \ddot{\phi}$$

$$(109) \quad H = T_H \cos (\gamma + \theta + \phi) - T_V \sin (\gamma + \theta + \phi)$$

$$+ FEL_{\gamma + \theta} \cos (\tau - \gamma - \theta - \phi)$$

$$- FEQ_{\gamma + \theta} \cos (\tau - \gamma - \theta - \phi) - [M_D \, R_D \sin (\bar{\beta} + \phi)] \, \ddot{\phi}$$

EVALUATION OF STATIC REACTIONS

Under static conditions, the forces B(t), BF, f_1 and f_2 shown in Figure 12a will be assumed equal to zero. Then,

$$\Sigma F_\eta = 0 = R(t) - W_A \sin(\gamma)$$

$$R(t) = W_A \sin(\gamma)$$

$$\Sigma F_\zeta = 0 = S_1 + S_2 - W_A \cos(\gamma)$$

$$S_1 + S_2 = W_A \cos(\gamma)$$

$$\Sigma M_{\text{Mass Center}} = 0 = S_1 (\bar{a}) - S_2 (\bar{b} - \bar{a}) - R(t) [\zeta_A - \zeta_2]$$

$$S_1 (\bar{a}) - S_2 (\bar{b} - \bar{a}) = W_A [\zeta_A - \zeta_2] \sin \gamma$$

Solving simultaneously

(110) $$S_2 = \frac{W_A [(\bar{a}) \cos \gamma - (\zeta_A - \zeta_2) \sin \gamma]}{\bar{b}}$$

(111) $$S_1 = W_A \cos \gamma - S_2$$

The force in both equilibrators is determined in the manner described in developing the basic model. Therefore,

(112) $$FEQ = 2 [PEQ - KEQ (LEL_\gamma - LEL_0)]$$

To define the static load in the elevating mechanism (which was considered approximately zero when developing Models A and B), an examination of Figures 11 and 12 shows that, for the tipping parts (M_A and M_B)

$$\Sigma M_T = 0 = W_A (\eta_{AO} \cos \gamma - \zeta_A \sin \gamma)$$

$$+ W_B (\eta_B \cos \gamma - \zeta_B \sin \gamma)$$

$$- FEQ_\gamma \cos \tau [\zeta_{EL}] - FEQ_\gamma \sin \tau [\eta_{EL}]$$

$$+ FEL_\gamma \sin \tau [\eta_{EL}] + FEL_\gamma \cos \tau [\zeta_{EL}]$$

Under static conditions, θ and ϕ are equal to zero. Therefore,

(113) $$\tau = \tan^{-1} \frac{Z_T + \eta_{EL} \sin \gamma + \zeta_{EL} \cos \gamma - Z_{EL}}{Y_{EL} - Y_T - \eta_{EL} \cos \gamma + \zeta_{EL} \sin \gamma} + \gamma$$

and the load in the elevating strut is given by

(114) $$FEL_\gamma = \frac{FEQ_\gamma (\eta_{EL} \sin \tau + \zeta_{EL} \cos \tau) - W_A (\eta_{AO} \cos \gamma - \zeta_A \sin \gamma) - W_B (\eta_B \cos \gamma - \zeta_B \sin \gamma)}{\eta_{EL} \sin \tau + \zeta_{EL} \cos \tau}$$

In a similar manner, the following equations allow for determination of the trunnion reactions.

$$\Sigma F_{\eta} = T_{H} - FEQ_{\gamma} \cos \tau + FEL_{\gamma} \cos \tau$$

$$- W_{A} \sin \gamma - W_{B} \sin \gamma$$

$$\Sigma F_{\zeta} = T_{V} + FEQ_{\gamma} \sin \tau - FEL_{\gamma} \sin \tau$$

$$- W_{A} \cos \gamma - W_{B} \cos \gamma$$

Therefore,

(115) $$T_{H} = (FEQ_{\gamma} - FEL_{\gamma}) \cos \tau + (W_{A} + W_{B}) \sin \gamma$$

(116) $$T_{V} = (W_{A} + W_{B}) \cos \gamma + (FEL_{\gamma} - FEQ_{\gamma}) \sin \tau$$

Finally, from Figure 11

$$\Sigma M_{O} = 0 = V_{spring} L - W_{A} [Y_{T} + \eta_{AO} \cos \gamma - \zeta_{A} \sin \gamma]$$

$$- W_{B} [Y_{T} + \eta_{B} \cos \gamma - \zeta_{B} \sin \gamma]$$

$$- W_{D} [Y_{D}]$$

$$\Sigma F_{H} = 0 = H$$

$$\Sigma F_{V} = 0 = V_{pivot} - W_{A} - W_{B} - W_{D} + V_{spring}$$

Therefore, under static conditions

(117) $H = 0$

(118) $$V_{spring} = \frac{W_A[Y_T + \eta_{AO} \cos \gamma - \zeta_A \sin \gamma] + W_B[Y_T + \eta_B \cos \gamma - \zeta_B \sin \gamma] + W_D Y_D}{L}$$

(119) $$V_{pivot} = W_A + W_B + W_D - V_{spring}$$

When the recoiling mass returns to the latch position at the end of any firing cycle or when it reaches the limit of forward travel in the case of a misfire, additional relative motion between the masses M_A and M_B is prevented by mechanical stops. Consequently, the preceding system of equations must be modified by eliminating Equation 91 completely and holding the value of η_A (and x) constant from this time on. At the same time, in the remaining equations,

$$\dot{\eta}_A = 0$$

$$\ddot{\eta}_A = 0$$

$$\mathrm{sgn}\ (\dot{\eta}_A) = 0$$

REFERENCES

1. GARVER, Harvey, "Final Report - An Investigation of the Firing Out Of Battery Principle on a Field Artillery Weapon", Report 64-1348, Research & Engineering Directorate, Rock Island Arsenal, April 1964.

2. TOWNSEND, Philip, "Analog Computer Study of the Initial Momentum Technique in Reducing Rod Pull Requirements for a 105mm Howitzer" Report 64-2615, Research & Engineering Directorate, Rock Island Arsenal, September 1964.

3. PETERSEN, Donald F., "Exploratory Development Studies of 105mm Fire Out Of Battery Weapon", Report 68-799, Research & Engineering Division, Rock Island Arsenal, March 1968.

4. SEAMANDS, Robert E., "Exploratory Development of Howitzer, Light, Towed; 105mm Soft Recoil, XM204", Artillery Systems Lab Report RE TR 70-179, Artillery Systems Laboratory, Research & Engineering Directorate, U. S. Army Weapons Command, Rock Island Arsenal, July 1970.

5. WHITCRAFT, James S., "Engineering Design Test of Howitzer, Light, Towed: 105mm Soft Recoil (Safety Certification)", Aberdeen Proving Ground Report APG-MT-3664, October 1970.

6. JOHNSTON, Major Franklin, Jr., "Military Potential Test of Howitzer, Light, Towed: 105mm Soft Recoil, XM204", U. S. Army Field Artillery Board, Final Report, 28 May 1971.

7. NERDAHL, Michael C. and FRANTZ, Jerry W., "Prediction of System Motion Based on a Simplified Mathematical Model for a Soft Recoil (Firing Out Of Battery) Mechanism", Technical Note Art 3-69, Research & Engineering Directorate, U. S. Army Weapons Command, May 1969.

8. NERDAHL, Michael C. and FRANTZ, Jerry W., "Engineering Analysis XM46 Recoil Mechanism, Design of Functional Controls and Prediction of System Motion", Artillery Systems Lab Report 69-1398 w/supplement, June 1969, Artillery Systems Laboratory, Research & Engineering Directorate, U. S. Army Weapons Command.

9. NERDAHL, Michael C. and FRANTZ, Jerry W., "Engineering Analysis, XM204 Howitzer (Soft Recoil), Effect of Carriage Flexibility on Weapon Response", Artillery Systems Lab Report RE 69-2779, Artillery Systems Laboratory, Research & Engineering Directorate, U. S. Army Weapons Command, December 1969.

10. GRITTON, Robert, "Initial Engineering Design and Test Effort on the XM204 Advanced Development Model", Technical Note A 2-71, Artillery and Air Defense Weapons Systems Directorate, Rock Island Weapons Laboratory, U. S. Army Weapons Command, August 1971.

SYMBOL TABLE

While symbols and subscripts have been defined (formally and/or pictorially) as they were introduced, the following list is included as a convenient reference. Model complexity, number of models, and use of standard notation has resulted in some symbol duplication. This table may aid in resolving questions resulting from such duplication. In all models, the basic units are:

inches
pounds
seconds
radians

A	Subscript showing relation to mass M_A	
A_1	Area at pressure P_1	Fig. 2
A_2	Area of spear buffer - pressure P_2	Figure 2
A_3	Area at pressure P_3	Figure 2
A_4	Effective area of floating piston (oil side)	Fig. 2
A_N	Effective area of floating piston (gas side)	Fig. 2
A_R	Area of each recoil rod	Fig. 2
A_B	Effective area of each front buffer piston	Fig. A-1
A(t)	Summation of forces causing positive accelerations	Fig. 7
a_1	Orifice area between pressures P_1 and P_2	Fig. 2
a_2	Orifice area between pressures P_2 and P_3	Fig. 2
a_3	Orifice area through velocity sensor. Effective area between pressures P_3 and P_4	Fig. 2
a_{3bf}	Value of a_3 before firing	
a_{3af}	Value of a_3 after firing	
a_v	Flow area through spear buffer check valve	Fig. 2 & 5

a_{leak}	Flow area due to clearance between spear buffer and piston head	Fig. 5
$a(x)$	Variable orifice area dependent on position of spear buffer	Fig. 5
a_B	Orifice area for front buffer	Fig. A-1
$\bar{\bar{a}}$	Locates centroid of area under B(t)	Figs. 8 & 9
$\bar{a}$	Distance from rear clip reaction to mass center of recoiling parts	Fig. 12 (a)
B	Subscript showing relation to mass M_B	
B	Measurement parallel to 0 - B axis	Fig. 11
BF	Retarding force of front buffer	
B(t)	Breech force	
$\bar{b}$	Distance between front and rear clip reactions	Fig. 12 (a)
C	Measurement parallel to 0 - C axis	Fig. 11
c_ϕ	Damping coefficient related to ϕ	
c_θ	Damping coefficicnet related to θ	
c_i	Discharge coefficient for orifice a_i	
D	Subscript showing relation to mass M_D	
D(t)	Summation of forces causing negative acceleration	Fig. 7
D_o	Value of D(t) at t = 0	Fig. 8
D_e	Value of D(t) at $t = t_R$	Fig. 8
D_r	Constant level for D(t) during recoil	Fig. 8
D_{CR}	Maximum value of D(t) during counterrecoil	Fig. 10

EQ	Subscript relating variable to equilibrator	
EL	Subscript relating variable to elevating struts	
F_ϕ	Generalized force (torque) causing rotation ϕ	
F_θ	Generalized force (torque) causing rotation θ	
FEL	Force on elevating struts	Fig. 12
FEQ	Force on equilibrators	Fig. 12
	NOTE: Elevating strut and equilibrator are considered to be separate but parallel units	
F_{fp}	Packing friction for floating piston	Fig. 2
F_p	Packing friction for recoil piston	Fig. 2
F_G	That portion of guide friction which is independent of clip reactions	Fig. 2
f_1	Guide friction due to clip reaction S_1	Fig. 12
f_2	Guide friction due to clip reaction S_2	Fig. 12
G	Subscript relating variable to ground spring or recoil guides	
g	Acceleration due to gravity	
$g(v_i)$	Pressure drop across 'i'th orifice	Eq. 1
H	Step function	Eq. 20
H	Horizontal reaction at ground pivot	Fig. 11
H	Constant related to elevating strut load	Fig. 15

I	Impulse - Area under B(t)	
I_A	Mass moment of inertia for M_A	
I_B	Mass moment of inertia for M_B	
I_D	Mass moment of inertia for M_D	
I.D.	Duration of ignition delay	
K	Spring rate for elevating struts	Fig. 15
K_{EQ}	Spring rate for equilibrator	Fig. 13
K_3	Spring rate of each front buffer return spring	Fig. A-1
K_G	Effective spring rate of ground spring	Fig. 11
k	Gas constant - Ratio of specific heats for gas at pressure P_N	
L	'Y' coordinate of ground spring	
LEL_0	Length of elevating struts at elevation = 0°	
LEL_γ	Length of elevating struts at initial elevation (γ)	
$LEL_{\gamma+\theta}$	Length of elevating struts at rotation θ	
M_R	Mass of recoiling parts without floating piston	Fig. 2
M_P	Mass of floating piston	Fig. 2
M_{eff}	Effective mass of recoiling parts	Eq. 27
M_A	Mass of recoiling parts used in three-degree-of-freedom model	Fig. 11, 12
M_B	Mass of elevating (but non-recoiling) portion of the weapon	Figs 11 & 12
M_D	Mass of non-elevating portion of the weapon	Fig. 11 & 16

N	Number of recoil cylinders	
O	Ground pivot - Origin of O - BC and O - YZ coordinate systems	Fig. 11
P_1	Oil pressure in recoil cylinder - spear buffer chamber	Fig. 2
P_2	Oil pressure in recoil rod	Fig. 2
P_3	Oil pressure in recoil cylinder	Fig. 2
P_4	Oil pressure in recuperator	Fig. 2
P_N	Gas pressure in recuperator	Fig. 2
P_o	Initial gas pressure in recuperator	Fig. 2
P_B	Oil pressure in front buffer	Fig. A-1
PEQ	Preload in equilibrator spring (i.e. - at $\gamma = 0°$)	
$\vec{Q}$	Vector locating mass center of recoiling parts	
$\vec{R}$	Vector locating mass center of elevating (but non-recoiling) parts	
R R(t)	Rod pull - Force on recoil rod	
R_D	Distance from ground pivot O to mass center of non-elevating parts	
r	Constant relating to elevating strut load	Fig. 15
S_1	Normal reaction at rear support of recoiling parts	Fig. 12
S_2	Normal reaction at front support of recoiling parts	Fig. 12
sgn(μ)	Algebraic sign of the variable μ	
S'	Preload in each front buffer return spring	

T	Elevation trunnion - origin of $T - \eta\ \zeta$ coordinate system	Fig. 11
T	Kinetic energy	
T	Duration of counterrecoil control function	Fig. 10
T_H	Trunnion reaction - $\parallel$ to $T - \eta$ axis	Fig. 12
T_V	Trunnion reaction - $\parallel$ to $T - \zeta$ axis	Fig. 12
t	Time variable	
t_r	Time of recoil	
t_f	Time of firing	
V	Potential energy	
V_{pivot}	Vertical reaction at pivot point O	Fig. 11
V_{spring}	Vertical reaction at ground spring	Fig. 11
V_N	Recuperator gas volume for displacement 'x'	
V_o	Initial recuperator gas volume ($x = 0$)	
v_i	Fluid velocity through 'i'th orifice	
W_R	Weight of reciling parts (without floating piston)	
W_p	Weight of floating piston	
W_{eff}	Effective weight of recoiling parts	Eq. 28
W_A	Weight of recoiling parts for three-degree-of-freedom model	
W_B	Weight of elevating (but non-recoiling) portion of weapon	
W_D	Weight of non-elevating parts	

$x, \dot{x}, \ddot{x}$	Displacement, velocity and acceleration of recoiling parts	Fig. 2
x_e	Recoil displacement for which spear buffer becomes effective	
x_v	Recoil displacement at which spear buffer check valve ceases to be effective	
x_{min}	Recoil displacement at which counterrecoil control by the spear buffer begins	
x_B	Recoil displacement at which front buffer is actuated	
$\dot{x}_{min}$	Constant counterrecoil velocity governed by flow through a_{3af}	
$\dot{x}_f$	Firing velocity	
x_T	Recoil displacement at which terminal counterrecoil velocity is reached	
$\dot{x}_T$	Terminal counterrecoil velocity	
Y	Measurement parallel to O - Y axis	Fig. 11
$y, \dot{y}, \ddot{y}$	Displacement, velocity and acceleration of floating piston	Fig. 2
Z	Measurement parallel to O - Z axis	Fig. 11
α	ζ coordinate of f_1	Fig. 12
β	ζ coordinate of f_2	Fig. 12
τ	Angle locating mass center of non-elevating parts	Fig. 16
γ	Initial angle of elevation	Fig. 11
Δ	Deflection of ring springs in elevating struts	Fig. 15

Δ_T	Specified rise and fall times for D(t)	Fig. 8
ζ	Measurement parallel to T - ζ axis	Fig. 11
η	Measurement parallel to T - η axis	Fig. 11
$\eta_A, \dot{\eta}_A, \ddot{\eta}_A$	Defines position, velocity, and acceleration of mass M_A with respect to the elevation trunnion	Fig. 12
η_{AO}	Initial value of η_A	
$\theta, \dot{\theta}, \ddot{\theta}$	Defines relative rotation, velocity and acceleration between M_B and M_D around the elevation trunnion	Fig. 11
μ	Coefficient of friction	
σ	Density of recoil oil	
τ	Angle between elevation strut and the T - η axis	Fig. 12
$\phi, \dot{\phi}, \ddot{\phi}$	Defines rotation, velocity and acceleration of mass M_D around an axis of rotation fixed in the ground at point O	Fig. 11

APPENDIX

MATHEMATICAL MODEL OF FRONT BUFFER

In case of a misfire or accidental tripping of the latch mechanism, the recoiling parts will be driven to their forward limit of travel. Consequently, a hydraulic buffer is incorporated in the design to bring the moving mass to rest and protect the weapon against impact loading. Since fluid flow from the recuperator is restricted after the velocity sensor has functioned, the front buffer design will be based on the maximum expected firing velocity. This mechanism is shown schematically in Figure A-1.

To limit the initial impact loading which occurs as the recoiling mass (M_R) hits the buffer pistons (M_B), a spring assembly (rate = K_1) was added to the recoiling parts. The spring rate was chosen so that the velocities of M_R and M_B are approximately equal when the spring deflection becomes equal to Δ . After this time, the resisting force of the front buffer is defined by:

$$BF = 2A_B P_B - 2\ K_3(x - x_B) + 2S'$$

where

S' = Preload in each buffer spring

K_3 = Spring rate of buffer spring

x_B = Recoil displacement for actuation of front buffer

A_B = Effective area of each buffer piston

P_B = Buffer oil pressure.

Now, the pressure drop across the orifice a_B is given by

$$\Delta P = \frac{\sigma}{2g} \frac{v_B^2}{c_B^2} \operatorname{sgn}(v_B)$$

and, since

$$A_B \dot{x} = - a_B v_B$$

$$\Delta P = - \frac{\sigma}{2g} \frac{A_B^2}{a_B^2} \dot{x}^2 \, \mathrm{sgn}(\dot{x})$$

Therefore,

$$BF = 2A_B \left[- \frac{\sigma}{2g} \right] \frac{A_B^2}{a_B^2} \dot{x}^2 \, \mathrm{sgn}(\dot{x}) - 2K_3 (x - x_B) + 2S'$$

$$BF = - \frac{\sigma}{g} \frac{A_B^3}{a_B^2} \dot{x}^2 \, \mathrm{sgn}(\dot{x}) - 2K_3 (x - x_B) + 2S'$$

NOTE: BF is effective only if $\dot{x} < 0$ and $x < x_B$ with $x_B \leq 0$

For a more complete description of a design procedure for this mechanism, see Reference 8, pages 97 - 117.

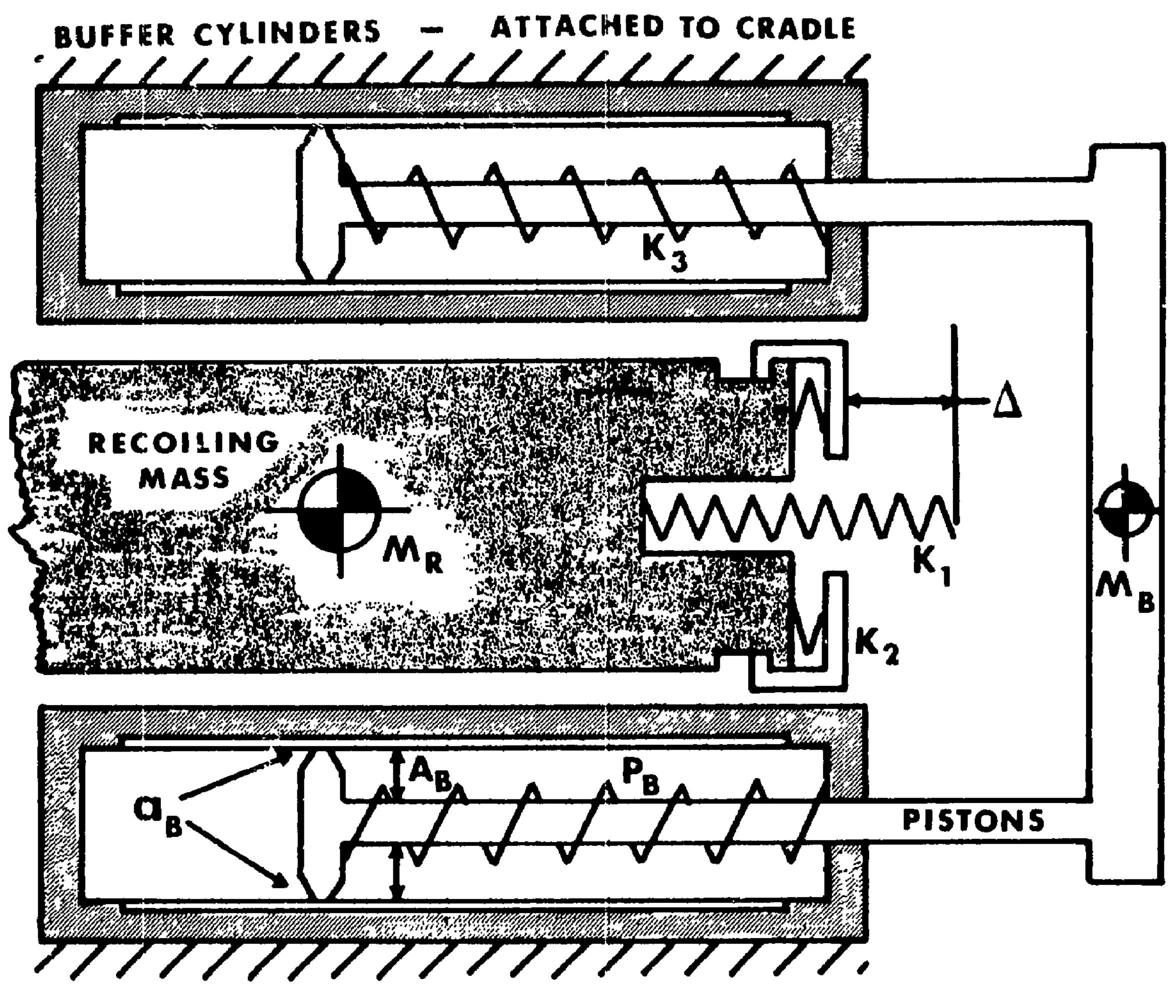

FIGURE A-1

Schematic Diagram of Forward Buffer

DISTRIBUTION

Department of the Army
Office, Assistant Chief of Staff for Force Development
Washington, D. C. 20310
1 ATTN: DAFD-SDF (LTC J. N. Hale)

Commander
Headquarters, U. S. Army Materiel Command
Washington, D. C. 20315
2 ATTN: AMCRD-WC

Commander
Headquarters, U. S. Army Combat Developments Command
Fort Belvoir, Virginia 22060
1 ATTN: CDCMR-W
1 ATTN: Technical Library

1 Commander
U. S. Army Combat Developments Command
Combat Systems Group
Fort Leavenworth, Kansas 66027

1 Commander
U. S. Army Combat Developments Command
Institute of Combined Arms & Support
Fort Leavenworth, Kansas 66027

Commander
Headquarters, U. S. Army Weapons Command
Rock Island, Illinois 61201
1 ATTN: AMSWE-RD
1 ATTN: AMSWE-RDP
1 ATTN: AMSWE-LCA
1 ATTN: AMSWE-LCD
1 ATTN: AMSWE-LMC
1 ATTN: AMCPM-CAWS

Commander
Headquarters, U. S. Army Test & Evaluation Command
Aberdeen Proving Ground, Maryland 21005
1 ATTN: AMSTE-FA

UNCLASSIFIED
Security Classification

DOCUMENT CONTROL DATA - R & D

(Security classification of title, body of abstract and indexing annotation must be entered when the overall report is classified)

1. ORIGINATING ACTIVITY (Corporate author) Artillery Weapons Systems Directorate Weapons Laboratory - Rock Island U. S. Army Weapons Command	2a. REPORT SECURITY CLASSIFICATION Unclassified 2b. GROUP NA

3. REPORT TITLE
Mathematical Models for Engineering Analysis and Design of Howitzer, Light, Towed; 105mm Soft Recoil, XM204

4. DESCRIPTIVE NOTES (Type of report and inclusive dates)
Summary Report (Jun 72 - May 73)

5. AUTHOR(S) (First name, middle initial, last name)
Michael C. Nerdahl & Jerry W. Frantz

6. REPORT DATE	7a. TOTAL NO. OF PAGES	7b. NO. OF REFS
May 1973	93	10

8a. CONTRACT OR GRANT NO. b. PROJECT NO. 1-W-5-63608-D-376 c. d.	9a. ORIGINATOR'S REPORT NUMBER(S) R-RRA-S-3-28-73 9b. OTHER REPORT NO(S) (Any other numbers that may be assigned this report) None

10. DISTRIBUTION STATEMENT
~~Distribution limited to U. S. Government agencies only; Test and Evaluation of military hardware presented; May 1973. Other requests for this document must be referred to Artillery Weapon Systems Directorate, Rock Island Weapons Laboratory~~

11. SUPPLEMENTARY NOTES	12. SPONSORING MILITARY ACTIVITY
None	U. S. Army Weapons Command

13. ABSTRACT

Mathematical models used in design of the XM204 Howitzer (AD and ED Prototypes) are described in this report. The physical basis for the mathematical representation is presented along with the derivation of the required equations. While these models have been generalized to allow their use in other weapon design situations, some modification will be necessary to include features not specifically considered. Systems of equations which will provide for the definition of required control functions as well as the prediction of recoil mechanism functioning and weapon motions are summarized.

DD FORM 1 NOV 65 1473 REPLACES DD FORM 1473, 1 JAN 64, WHICH IS OBSOLETE FOR ARMY USE.

UNCLASSIFIED
Security Classification

14. KEY WORDS	LINK A		LINK B		LINK C	
	ROLE	WT	ROLE	WT	ROLE	WT
Artillery XM204 Howitzer Design Mathematical Model Soft Recoil Mechanism Design						

AD ____________ ACCESSION NO. ________
Artillery Weapons Systems Directorate,
Rock Island Weapons Laboratory, U. S. Army
Weapons Command

MATHEMATICAL MODELS FOR ENGINEERING ANALYSIS
AND DESIGN OF HOWITZER, LIGHT, TOWED; 105mm
SOFT RECOIL, XM204
by Michael C. Nerdahl & Jerry W. Frantz

Technical Report R-RRA-S-3-28-73
May 1973
93 pages, including drawings and figures
Unclassified report

Mathematical models used in design of the XM204 Howitzer (AD and ED Prototypes) are described in the report. The physical basis for the mathematical representation is presented along with the derivation of the required equations. While these models have been generalized to allow their use in other weapon design situations, some modification will be necessary to include features not specifically considered. Systems of equations which will provide for the definition of required control functions as well as the prediction of recoil mechanism functioning and weapon motions are summarized.

UNCLASSIFIED

1. Artillery
2. XM204 Howitzer Design
3. Mathematical Model
4. Soft Recoil Mechanism Design

I. Michael C. Nerdahl & Jerry W. Frantz
II. U. S. Army Weapons Command
III. Rock Island Weapons Laboratory, Artillery Weapons Systems Directorate

DISTRIBUTION

Copies obtainable from
Defense Documentation Center

UNCLASSIFIED

AD ____________ ACCESSION NO. ________
Artillery Weapons Systems Directorate,
Rock Island Weapons Laboratory, U. S. Army
Weapons Command

MATHEMATICAL MODELS FOR ENGINEERING ANALYSIS
AND DESIGN OF HOWITZER, LIGHT, TOWED; 105mm
SOFT RECOIL, XM204
by Michael C. Nerdahl & Jerry W. Frantz

Technical Report R-RRA-S-3-28-73
May 1973
93 pages, including drawings and figures
Unclassified report

Mathematical models used in design of the XM204 Howitzer (AD and ED Prototypes) are described in the report. The physical basis for the mathematical representation is presented along with the derivation of the required equations. While these models have been generalized to allow their use in other weapon design situations, some modification will be necessary to include features not specifically considered. Systems of equations which will provide for the definition of required control functions as well as the prediction of recoil mechanism functioning and weapon motions are summarized.

UNCLASSIFIED

1. Artillery
2. XM204 Howitzer Design
3. Mathematical Model
4. Soft Recoil Mechanism Design

I. Michael C. Nerdahl & Jerry W. Frantz
II. U. S. Army Weapons Command
III. Rock Island Weapons Laboratory, Artillery Weapons Systems Directorate

DISTRIBUTION

Copies obtainable from
Defense Documentation Center

UNCLASSIFIED

AD ____________ ACCESSION NO. ________
Artillery Weapons Systems Directorate,
Rock Island Weapons Laboratory, U. S. Army
Weapons Command

MATHEMATICAL MODELS FOR ENGINEERING ANALYSIS
AND DESIGN OF HOWITZER, LIGHT, TOWED; 105mm
SOFT RECOIL, XM204
by Michael C. Nerdahl & Jerry W. Frantz

Technical Report R-RRA-S-3-28-73
May 1973
93 pages, including drawings and figures
Unclassified report

Mathematical models used in design of the XM204 Howitzer (AD and ED Prototypes) are described in the report. The physical basis for the mathematical representation is presented along with the derivation of the required equations. While these models have been generalized to allow their use in other weapon design situations, some modification will be necessary to include features not specifically considered. Systems of equations which will provide for the definition of required control functions as well as the prediction of recoil mechanism functioning and weapon motions are summarized.

UNCLASSIFIED

1. Artillery
2. XM204 Howitzer Design
3. Mathematical Model
4. Soft Recoil Mechanism Design

I. Michael C. Nerdahl & Jerry W. Frantz
II. U. S. Army Weapons Command
III. Rock Island Weapons Laboratory, Artillery Weapons Systems Directorate

DISTRIBUTION

Copies obtainable from
Defense Documentation Center

UNCLASSIFIED

AD ____________ ACCESSION NO. ________
Artillery Weapons Systems Directorate,
Rock Island Weapons Laboratory, U. S. Army
Weapons Command

MATHEMATICAL MODELS FOR ENGINEERING ANALYSIS
AND DESIGN OF HOWITZER, LIGHT, TOWED; 105mm
SOFT RECOIL, XM204
by Michael C. Nerdahl & Jerry W. Frantz

Technical Report R-RRA-S-3-28-73
May 1973
93 pages, including drawings and figures
Unclassified report

Mathematical models used in design of the XM204 Howitzer (AD and ED Prototypes) are described in the report. The physical basis for the mathematical representation is presented along with the derivation of the required equations. While these models have been generalized to allow their use in other weapon design situations, some modification will be necessary to include features not specifically considered. Systems of equations which will provide for the definition of required control functions as well as the prediction of recoil mechanism functioning and weapon motions are summarized.

UNCLASSIFIED

1. Artillery
2. XM204 Howitzer Design
3. Mathematical Model
4. Soft Recoil Mechanism Design

I. Michael C. Nerdahl & Jerry W. Frantz
II. U. S. Army Weapons Command
III. Rock Island Weapons Laboratory, Artillery Weapons Systems Directorate

DISTRIBUTION

Copies obtainable from
Defense Documentation Center

UNCLASSIFIED